AD-A080 108 PHYSICAL SCIENCES INC WOBURN MASS F/G 20/4
REMOTE MEASUREMENT OF DENSITY FLUCTUATIONS IN TURBULENT FLOWS.(U)
AUG 79 J S GOELA, T F MORSE, L G PIPER F49620-78-C-0099
UNCLASSIFIED PSI-TR-189 AFOSR-TR-80-0027 NL

1 OF 1
AD A080108

END
DATE FILMED
3 - 80
DDC

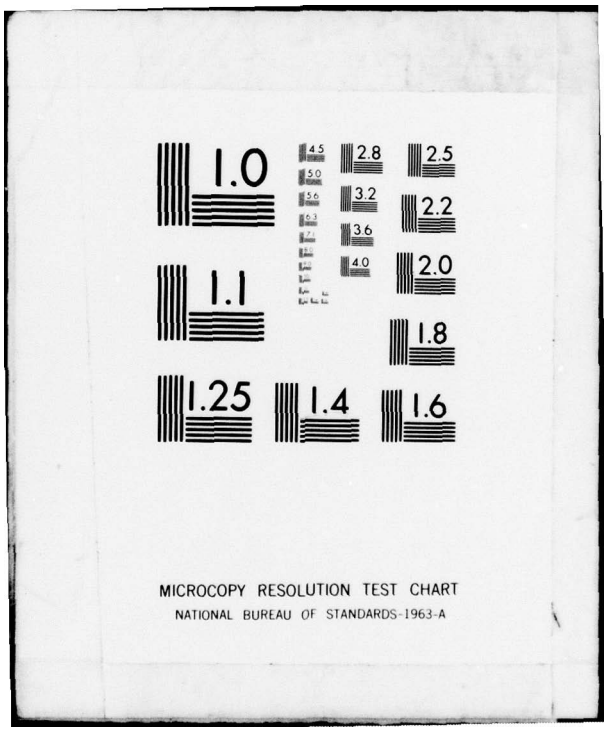
1.0
1.1
1.25
1.4
1.6
1.8
2.0
2.2
2.5
2.8
3.2
3.6
4.0
4.5
5.0
5.6
6.3
MICROCOPY RESOLUTION TEST CHART
NATIONAL BUREAU OF STANDARDS-1963-A

0-0027

TR-189

3 LEVEL II

REMOTE MEASUREMENT OF DENSITY FLUCTUATIONS IN TURBULENT FLOWS

by

J. S. Goela, T. F. Morse* and
L. G. Piper

Prepared for

The Air Force Office of Scientific Research
Bolling Air Force Base
Washington, D. C.

Final Report

under

Contract No. F 49260-78-C-0099

August 1, 1979

*Division of Engineering, Brown University, Providence, R.I. 02912

PHYSICAL SCIENCES INC.
30 COMMERCE WAY, WOBURN, MASS. 01801

UNCLASSIFIED

SECURITY CLASSIFICATION OF THIS PAGE (When Data Entered)

REPORT DOCUMENTATION PAGE	READ INSTRUCTIONS BEFORE COMPLETING FORM
1. REPORT NUMBER: AFOSR-TR-80-0027	2. GOVT ACCESSION NO. / 3. RECIPIENT'S CATALOG NUMBER
4. TITLE (and Subtitle): REMOTE MEASUREMENT OF DENSITY FLUCTUATIONS IN TURBULENT FLOWS.	5. TYPE OF REPORT & PERIOD COVERED: FINAL rept. 1 Aug 78 — 31 Jul 79
	6. PERFORMING ORG. REPORT NUMBER
7. AUTHOR(s): J. S. GOELA, T. F. MORSE, L. G. PIPER	8. CONTRACT OR GRANT NUMBER(s): F49620-78-C-0099
9. PERFORMING ORGANIZATION NAME AND ADDRESS: PHYSICAL SCIENCES INC, 30 COMMERCE WAY, WOBURN, MA 01801	10. PROGRAM ELEMENT, PROJECT, TASK AREA & WORK UNIT NUMBERS: 2307A3, 61102F
11. CONTROLLING OFFICE NAME AND ADDRESS: AIR FORCE OFFICE OF SCIENTIFIC RESEARCH/NA, BLDG 410, BOLLING AIR FORCE BASE, D C 20332	12. REPORT DATE: 1 Aug 79
	13. NUMBER OF PAGES: 73
14. MONITORING AGENCY NAME & ADDRESS (if different from Controlling Office): PSI-TR-189	15. SECURITY CLASS. (of this report): UNCLASSIFIED
	15a. DECLASSIFICATION/DOWNGRADING SCHEDULE

16. DISTRIBUTION STATEMENT (of this Report)

Approved for public release; distribution unlimited.

17. DISTRIBUTION STATEMENT (of the abstract entered in Block 20, if different from Report)

18. SUPPLEMENTARY NOTES

19. KEY WORDS (Continue on reverse side if necessary and identify by block number)

LAWER APPLICATIONS
REMOTE MONITORING
TURBULENCE
REMOTE MEASUREMENTS
LASERS

20. ABSTRACT (Continue on reverse side if necessary and identify by block number)

This report describes the results of a theoretical study carried out to explore the possibility of obtaining quantitative information about density fluctuations in an air turbulent flow. Specific techniques considered for analysis include a new three-level gain measurement technique, the use of laser induced gas breakdown as a diagnostic tool, and monitoring of the laser induced fluorescence signal. The effect of turbulence on the diagnostic design is considered and the possibility of conducting a laboratory experiment with the use of commercially available lasers is discussed.

DD FORM 1 JAN 73 1473 EDITION OF 1 NOV 65 IS OBSOLETE

UNCLASSIFIED

ABSTRACT

This report describes the results of a theoretical study carried out to explore the possibility of obtaining quantitative information about density fluctuations in an air turbulent flow. Specific techniques considered for analysis include a new three-level gain measurement technique, the use of laser induced gas breakdown as a diagnostic tool, and monitoring of the laser induced fluorescence signal. The effect of turbulence on the diagnostic design is considered and the possibility of conducting a laboratory experiment with the use of commercially available lasers is discussed.

This manuscript is submitted for publication with the understanding that the United Stated Government is authorized to reproduce and distribute reprints for governmental purposes.

TABLE OF CONTENTS

LIST OF ILLUSTRATIONS

LIST OF TABLES

ACKNOWLEDGEMENTS

Sponsorship Statement

Research sponsored by the Air Force Office of Scientific Research (AFSC), United States Air Force, under Contract #F49620-78-C-0099. The United States Government is authorized to reproduce and distribute reprints for governmental purposes notwithstanding any copyright notation hereon.

1. INTRODUCTION

The purpose of this study is to investigate new techniques for monitoring density fluctuations in a turbulent flow field; in particular, a new three-level gain measurement scheme is examined with the aim of providing important information about the turbulent flow field behind a turret mounted on an airplane. For this application there are certain constraints under which the density diagnostic is to function. These constraints include a spatial resolution of approximately 1 cm, and the capability of monitoring 1% density fluctuations non-intrusively, instantaneously, accurately and remotely.

Several schemes, which may be used to monitor species concentrations in a flow field, are available,[1-11] but all these schemes suffer from one or more drawbacks. Methods involving shadowgraph, schlieren, interferometry and resonance absorption of light can only provide information about the average density along a given path length. Scattering techniques based upon Raman and Rayleigh processes, in principle, can provide the necessary spatial and temporal resolution needed to make such measurements in a turbulent environment; however, Raman scattering cross-sections are small with the result that a reasonably good signal to noise ratio is difficult to obtain, while the Rayleigh scattered signal may contain significant contributions from Mie scattering. Furthermore, under combustion conditions, Robben[11] has concluded that for the measurement of 10% root mean square turbulent fluctuations or less, the Raman scattering technique is incapable of making a satisfactory measurement.

Recently, Daily[5] has used laser induced fluorescence to measure density in turbulent reacting flows. An important feature of his technique is that if a laser is used to saturate a particular transition, the fluorescence signal from the excited state is independent of the quenching rates. The possibility of using this technique to measure density fluctuations has also been explored in this report in Section 3.

The main emphasis in this report is the theoretical evaluation of a three-level gain measurement technique as a possible method for obtaining quantitative information about density fluctuations in an air turbulent boundary layer. Several naturally occurring species in the atmosphere can be used to make such a measurement and details about three-level gain measurements are provided in Section 2. In Section 3, techniques for monitoring other parameters which can be related to gas density are considered. These techniques include monitoring laser induced fluorescence and the use of gas breakdown as a diagnostic tool. In Section 4, the effect of turbulence on diagnostic design is discussed, and the possibility of conducting a laboratory experiment to test the diagnostic scheme is explored in Section 5. Finally, the conclusions are presented in Section 6.

2. THREE-LEVEL GAIN MEASUREMENT TECHNIQUES

The basic three-level gain measurement scheme entails using a high power pulsed laser to saturate one transition of a molecule and measuring gain on a coupled transition of the same molecule with a probe laser. As shown in Fig. 1, the pump laser saturates the transition $1 \leftrightarrow 2$ while the probe laser measures gain on transition $2 \leftrightarrow 3$. The power of the pump laser is chosen such that in each shot the transition is saturated even though there may be variations in the output of the pump laser from shot to shot. This condition is realized when the pump laser intensity is always greater than the saturation intensity for the transition; consequently, pump laser variations play no role.

Saturating transition $1 \leftrightarrow 2$ means that a specified number of molecules (and this number can be calculated) will be excited from level 1 to level 2. Measurement of small signal gain on transition $2 \leftrightarrow 3$ can provide quantitative information about the number of particles in level 2. This in turn is related to the total concentration of the species through the saturation condition. Now, if the concentration of the species involved in a gain measurement in the atmosphere is known, we can determine the atmospheric density. To obtain good spatial resolution required for making measurements in a turbulent environment, the pump and probe lasers are placed in a perpendicular configuration as illustrated in Fig. 2.

A list of naturally present species, along with their atmospheric concentrations, is given in Table 1. It can be seen that there are several species which might be suitable for a gain measurement. Selection of a species, however, depends upon a number of criteria including (a) the availability of a high power laser having a lasing frequency resonant with the transition frequency of interest in the chosen molecule, (b) measurable amount of gain obtainable on the coupled transition, and, (c) availability of a probe laser of sufficient intensity to measure the gain. There are very few high power lasers available in the visible and

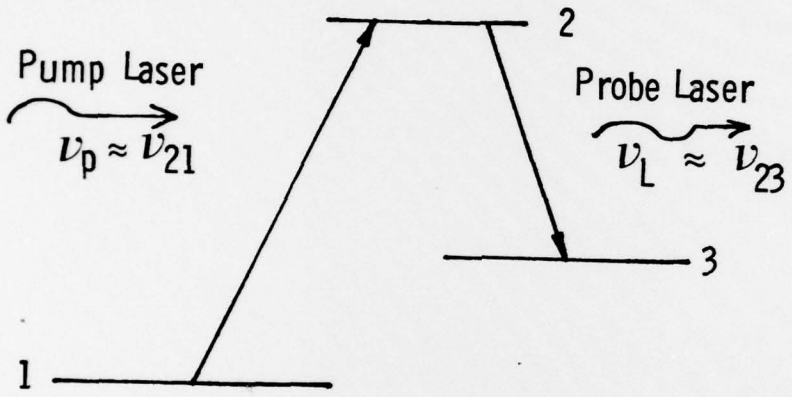

Fig. 1 The basic three level gain measurement scheme.

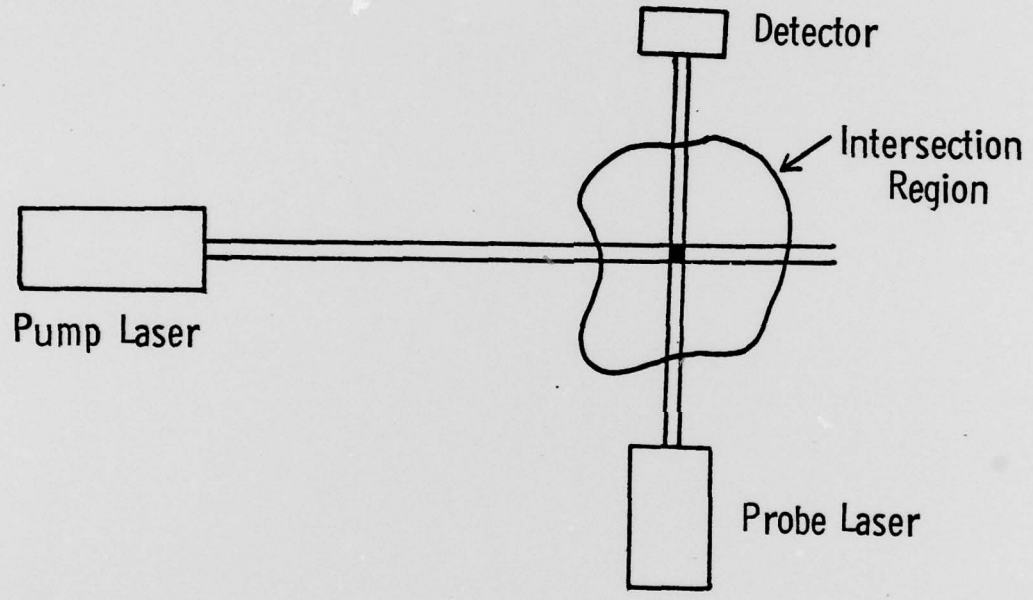

Fig. 2 Arrangement of Pump and Probe lasers in the three level scheme to make spatially resolved measurements.

TABLE 1.

Concentration of Gases in Air

Constituent	ppm by Volume
N_2	7.808×10^5
O_2	2.09×10^5
H_2O*	2.5×10^4
A	9.34×10^3
CO_2	330
Ne	18.18
He	5.24
CH_4	1.6
Kr	1.14
H_2	0.5
N_2O	0.28
Xe	0.087
CO	0.075

*For tropical atmospheres at sea level.

UV. This means that saturating an electronic transition is perhaps not practical. Ideally, one would like to work with nitrogen or oxygen because these gases have appreciable concentrations in the atmosphere. However, there are no laser frequencies which are resonant with the two coupled allowed transitions in these molecules.

The amount of water vapor in the atmosphere varies, and for tropical atmospheres at sea level, the water vapor concentration is 2.5% by volume. The water molecule is one of the molecules which has been investigated in this study for a possible three-level gain measurement. Another molecule considered is CO_2, which has a concentration of .03% by volume. Argon and other inert gases have not been studied because electronic transitions are involved. Methane, N_2O and other trace gases are possible candidates for a three-level gain measurement, but their concentration in the atmosphere is too small to produce an appreciable gain necessary for an accurate measurement of density.

2.1 Three-Level Gain Measurement in CO_2

In the lowest electronic state of CO_2 there are several coupled transitions involving vibrational levels which can be employed for a three-level measurement. However, the suitability of a particular transition for making a density measurement depends upon the availability of lasers. With the use of the existing commercially available laser systems, the three-level gain measurement in CO_2 may be made in the following three ways: (i) 2.7 μm HF laser pumping of the 000 ↔ 021 or 000 ↔ 011 transition and gain measurement on the 021 ↔ 020 transition with a 4.3 μm CW diode laser; (ii) 4.3 μm HBr laser pumping of the 000 ↔ 001 transition and gain measurement on the 001 ↔ 100 transition with a 10.6 μm CO_2 probe laser; and, (iii) pumping of the 000 ↔ 001 transition with a 4.3 μm HBr laser and gain measurement on the 001 ↔ 000 transition with a 4.3 μm CW diode laser.

Detailed theoretical calculations have been made and these calculations show that scheme (i) is the most promising of the three schemes outlined above. Consequently, in the following we will discuss scheme (i) in detail, while the other two schemes will be described only briefly.

The vibrational levels 021 and 011 of CO_2 are in Fermi resonance. Therefore, we assume that these two levels are in equilibrium at all times. Several HF laser lines are in near resonance with different rotational lines of combination bands 000 $\leftrightarrow$ 021 and 000 $\leftrightarrow$ 011 in CO_2. The selection of a particular HF laser line is based upon the following criterion:

(a) The HF laser line should be in resonance with a high J rotational line on an R-branch transition. Theoretical calculations given in Appendix II show that when a high intensity laser is resonant with a high J rotational line in an R-branch transition, it is possible to excite more than half of the ground state particles to the excited vibrational manifold;*

(b) The HF laser line selected for pumping must be one of the stronger lines of the HF laser to achieve the necessary saturation condition;

(c) The laser intensity needed to cause saturation should be such that it must not cause breakdown in the air.

After taking into consideration the above criterion, it turns out that the P(4) line of the transition 2 $\leftrightarrow$ 1 in an HF laser is best suited to saturate the 000 $\leftrightarrow$ 021 transition in CO_2. The P(4) line (ν_p = 3622.663 cm^{-1}) is in near resonance with the R(12) line (ν_p = 3622.492 cm^{-1}) of the 100 $\leftrightarrow$ 021 transition in CO_2. The exact frequencies of HF laser lines are taken from Ref. 12 while the frequency and the strength of rotational lines in a particular band of CO_2 are obtained from a computer program which uses the parameters compiled in Ref. 13.

*To be published in Optics Letters, December 1979.

The laser intensity required to saturate a transition can be calculated from Eq. (AI-10) derived in Appendix I. To calculate saturation intensity one needs the characteristic time for vibrational relaxation (τ_v), the Einstein coefficient, (A), for vibration-rotation transitions corresponding to the R(12) line of the 000 $\leftrightarrow$ 021 transition in CO_2 and the width ($\Delta\nu_L$) of the rotational line R(12). The vibrational relaxation time constant (τ_v) for level 021 has been taken to be the characteristic time for the V-V transfer process which is the fastest rate of deactivation of the 021 level in CO_2.

$$CO_2\ (021) + N_2\ (v = 0) \rightarrow CO_2\ (020) + N_2\ (v = 1).$$

The rate constant for this reaction is[14] 1.6×10^6 sec^{-1}. Consequently, $\tau_v = 6 \times 10^{-7}$ sec. Other deactivation rates for the excited level 021 are much smaller and the value 6×10^{-7} sec should be correct to within a factor of 2 of the true value of τ_v.

The Einstein coefficient for the particular vibration-rotation transition has been calculated from the following relation:

$$A = \left(\frac{2.8}{\lambda^2}\right) S\ (2.48 \times 10^{19})\ \exp\ (\nu_L'\ 1.4387/T)\ , \qquad (1)$$

where

S = Line strength in $\left(\frac{cm^{-1}}{cm^{-2}}\ molecule^{-1}\right)$ obtained from a computer program based upon parameters of Ref. 13.

λ = Transition wavelength in μm.

ν_L' = Energy of the lower level in cm^{-1}.

For the R(12) line of 000 $\leftrightarrow$ 021 transition in CO_2,

$$S = 1.035 \times 10^{-18} \left(\frac{cm^{-1}}{cm^{-2}} \text{ molecule}^{-1} \right), \nu_L' = 0,$$

$$T = 300 \text{ K}, \lambda = 2.76 \text{ } \mu m.$$

Substituting these values into Eq. (1) we find $A = 9.38 \text{ sec}^{-1}$.

The width, $\Delta\nu_L$, of the rotational line R(12) has been taken to be the mean full width at half maximum of the CO_2 molecule at 1 atmosphere pressure as listed in Ref. 13 ($\Delta\nu_L = 0.07 \text{ cm}^{-1}$).

Substituting the value of τ_v, A, and $\Delta\nu_L$ in Eq. (AI-10), we find that the laser intensity required to saturate the R(12) line in CO_2 must be much greater than 0.185 MW/cm^2. To saturate the vibrational transition 000 $\leftrightarrow$ 021 completely, however, this intensity must be divided by the Boltzmann factor for the R(12) line (see Appendix I). Taking into account the Fermi resonance between levels 021 and 011, the Boltzmann factor for the R(12) line is 0.0173. Therefore, the laser intensity needed to saturate the vibrational band 000 $\leftrightarrow$ 021 must be much greater than 11 MW/cm^2. Thus, tens of MW/cm^2 of laser power will be required to saturate the combination band 000 $\leftrightarrow$ 021.

A laser intensity of tens of megawatts per square cm at 2.7 μm does not cause breakdown in clean air. Even when the air is mixed with particulate matter, there will be no breakdown in air at 2.7 μm if the laser pulse duration is 1 μsec or shorter. The choice of the laser pulse duration, τ_p, depends upon τ_v ($\tau_p \leq \tau_v$). Since τ_v = .6 μsec, the whole experiment will be completed in less than 1 μsec. Thus, under experimental conditions of interest to us, air breakdown should not occur.

2.2 Calculation of the Absorption Coefficient

The knowledge of the absorption coefficient in air at the pump laser frequency is necessary to determine how far along the path the laser beam will be able to saturate the gas. The absorption coefficient in cm^{-1} has been calculated using the following relation:

$$\kappa(\nu) = \frac{S\,\Delta\nu_L\,N}{2\pi\left[(\nu_p - \nu_o)^2 + \left(\frac{\Delta\nu_L}{2}\right)^2\right]} \qquad (2)$$

where

S = Line strength in (cm molecule^{-1}).

N = Number density of absorbers, cm^{-3}.

ν_p = Pump laser frequency, cm^{-1}.

ν_o = Line center frequency of the transition, cm^{-1}.

$\Delta\nu_L$ = Full width at half maximum, cm^{-1}.

For the HF laser line P(4) $2 \rightarrow 1$, $S = 1.035 \times 10^{-18}$ cm molecule^{-1}, $N = 7.35 \times 10^{15}$ molecules/cm^3 at sea level, $(\nu_p - \nu_o) = 0.171\ cm^{-1}$ and $\Delta\nu_L = 0.07\ cm^{-1}$. Substituting these values in Eq. (2), we get $\kappa(\nu_p) = 1.71 \times 10^{-4}\ cm^{-1}$. Thus, the HF laser will be able to saturate the 000 $\leftrightarrow$ 021 combination band in CO_2 over a path length of several meters in air.

2.3 Calculation of Small Signal Gain

Thus far we have concentrated on the calculation of pump laser parameters such as laser intensity, pulse duration and laser

absorption coefficient in air required to saturate the 000 ↔ 021 combination band in CO_2. By selecting an appropriate rotational line we have also tried to maximize the number of particles excited to the 021 level in CO_2. Now we concentrate on the calculation of probe laser parameters and on the maximization of gain on the coupled transition 021 ↔ 020.

In a thermalized rotational distribution, the gain on a P-branch transition is larger than on Q- or R-branch transitions. Consequently, for a given rotational partition function, the maximum gain is obtained when the rotational level with the most particles in the excited state is involved in the P-branch transition. On the coupled transition 021 ↔ 020 in CO_2, the P(16) line with frequency 2314.22 cm^{-1} will give the maximum gain. To measure this gain, a CW diode laser will be used. This laser can be fine tuned to match exactly the P(16) line of CO_2 on the 021 ↔ 020 transition.

The small signal gain, G, on the P(16) line of the 021 ↔ 020 transition in CO_2 has been calculated using the following expression:

$$G(\nu_L) = \frac{\lambda^2 A_J \Delta N_J}{4\pi^2 \Delta\nu_L \left[1 + 4\left(\frac{\nu_L - \nu_o}{\Delta\nu_L}\right)^2\right]} \qquad (3)$$

where ΔN_J is the population inversion on the P(16) line, A_J is the Einstein coefficient for spontaneous emission, ν_L is the frequency of the probe laser, and the other symbols have been defined previously.

The population inversion ΔN_J is calculated assuming that saturation with the pump laser will place approximately one third of the total molecules in the 021 level because there is Fermi resonance between levels 021 and 011. Substituting the values $\Delta N_J = 7.35 \times 10^{15} \times .33 \times .0369 = 8.95 \times 10^{13}$ molecules/cm^3, $A_J = 173$ sec^{-1}, $\Delta\nu_L = 0.07$ cm^{-1}, $(\nu_L - \nu_o) \approx 0$ and $\lambda = 4.32$ μm in Eq. (3), we get $G(\nu_L = 4.32\ \mu m) = 0.017$ cm^{-1}.

Measurement of gain at 2314.22 cm^{-1} (4.32 μm) may become difficult if there is appreciable absorption of the probe laser in air. The 4.3 μm band in CO_2 originating from the ground state is very strong. However, the frequency 2314.22 cm^{-1} is appreciably shifted from any of the vibration-rotation lines in the CO_2 000 ↔ 001 band. To see how much power the probe laser will lose as a consequence of this absorption, we calculate the absorption coefficient in air at 2314.22 cm^{-1} from Eq. (2). This absorption coefficient comes out to be 7.5×10^{-4} cm^{-1}. Thus, the probe laser can traverse a distance of several meters without appreciable attenuation in the air.

In summary, therefore, the three-level gain measurement technique involving the 021 ↔ 000 combination band in CO_2 yields a gain of 0.017 cm^{-1} with the use of commercially available laser systems. In Section IV, we will see whether a gain of 0.017 cm^{-1} is sufficient to provide quantitative information about turbulent density fluctuations in atmosphere. For convenience, first we summarize in Fig. 3 the salient features of the 4.3 μm gain measurement on 021 ↔ 000 transition.

Now let us briefly consider other techniques for making a three-level gain measurement in CO_2. One scheme involves pumping the 000 ↔ 001 transition in CO_2 with a 4.3 μm HBr laser and a gain measurement on the 001↔100 transition with a 10.6 μm CO_2 probe laser. The pump and probe laser requirements and other salient features of this scheme are summarized in Fig. 4. Calculations of the various parameters have been made following the procedure outlined above. From Fig. 4, it can be seen that one can only get a gain of 2×10^{-4} cm^{-1} which is much smaller than the gain of 0.017 cm^{-1} obtained from 021 ↔ 020 transition considered above.

Another three-level gain measurement in CO_2 involves pumping the 000 ↔ 001 transition with a 4.3 μm HBr laser and a gain measurement on the same 001 ↔ 000 transition with a 4.3 μm CW diode laser. This technique is based upon the fact that under certain conditions (which are specified in Appendix II), optically pumping an R-branch transition at high J number leads to gain at those frequencies which are smaller than the pump laser frequency. For this scheme, the pump and probe laser requirements are given In Fig. 5. It can be seen that this scheme is not

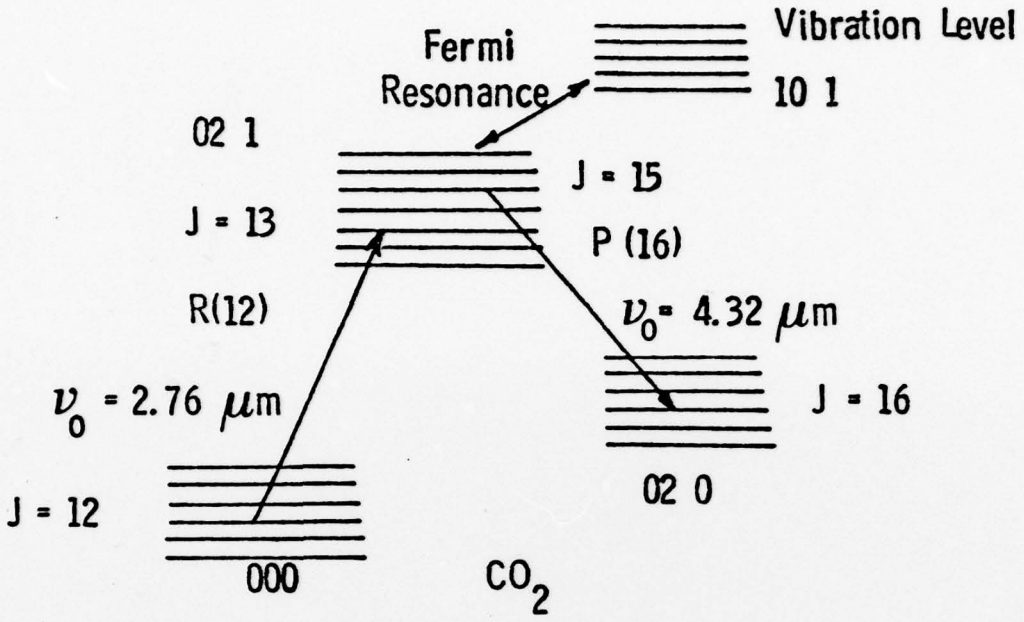

	Pump Laser Characteristics	Probe Laser Characteristics
Type	HF Pulsed Laser	CW Diode Laser
Laser frequency	2.76 μm, (2 → 1, P(4))	4.32 μm
Absorption/Gain line	CO_2, 000 ↔ 021, R(12)	CO_2, 021 ↔ 020, P(16)
Saturation intensity	> 10 MW/cm^2	---
Pulse duration	≤ 0.6 μsec	CW
Laser fluence	> 6 J/cm^2	---
Atmospheric absorption coefficient	1.71 x 10^{-4} cm^{-1}	7.5 x 10^{-4}
Gain at 4.32 μm	---	0.017 cm^{-1}

Fig. 3 Salient features of 4.3 μm gain measurement on hot band (021 ↔ 020) in CO_2.

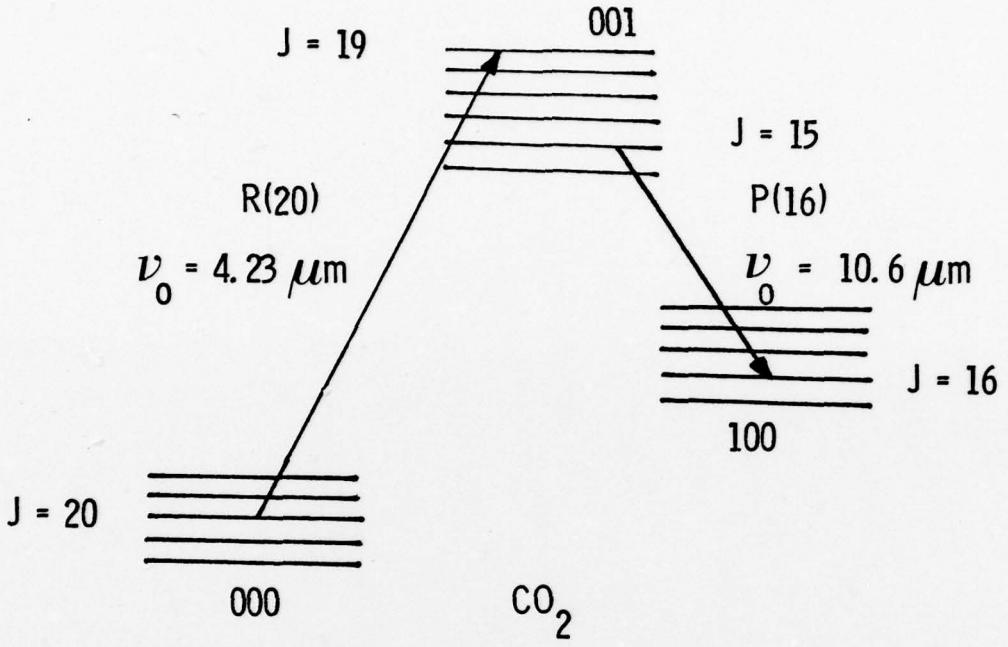

	Pump Laser Characteristics	Probe Laser Characteristics
Type	HBr Pulsed Laser	CW CO_2 Laser
Laser frequency	4.23 μm (2 → 1, P(6))	10.6 μm
Absorption/Gain Line	CO_2, 000 ↔ 100, R(20)	CO_2, 001 ↔ 100, P(16)
Satulation intensity	> 0.11 MW/cm^2	---
Atmospheric absorption coefficient	0.03 cm^{-1}	≈ 0
Pulse duration	≤ 0.6 μ sec	CW
Gain at 10.6 μm	---	2 x 10^{-4} cm^{-1}

Fig. 4 Salient features of 10.6 μm gain measurement in CO_2.

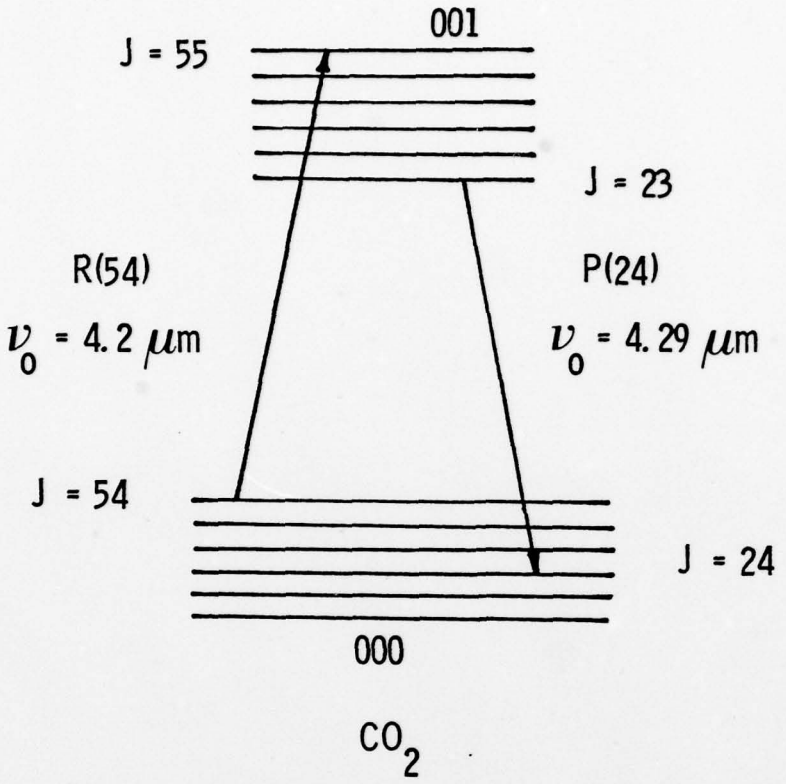

	Pumped Laser Characteristics	Probe Laser Characteristics
Type	HBr Pulsed Laser	CW Diode Laser
Laser frequency	4.2 μm (2 → 1, P(5))	4.29 μm
Absorption/Gain line	CO_2, 000 ↔ 001, R(54)	CO_2, 000 ↔ 001, P(24)
Saturation intensity	> 1.87 MW/cm^2	---
Atmospheric absorption coefficient	1.9 x 10^{-3} cm^{-1}	0.46 cm^{-1}
Gain at 4.29 μm	---	7.67 x 10^{-3} cm^{-1}
Pulse duration	≤ 0.6 μsec	CW

Fig. 5 Salient features of 4.3 μm gain measurement in CO_2 on 000 ↔ 001 band.

suitable for our application due to two reasons. First, the gain obtainable on the 001 ↔ 000 transition is only 7.67×10^{-3} cm^{-1}, which is smaller than the gain of 0.017 cm^{-1} obtainable from the 021 ↔ 020 transition considered above. Secondly, the probe laser absorption coefficient in the air is very high (= 0.46 cm^{-1}), with the result that most of the energy in the probe laser will be absorbed in the atmosphere by the time the probe laser reaches the detector.

2.4 Three-Level Gain Measurement in Water Vapor

The amount of water vapor in the atmosphere varies with the altitude, geographic location and the time of the year. For tropical atmospheres at sea level, the water vapor concentration is 2.5% by volume.[13] This concentration is approximately 8 times the concentration of CO_2 in the atmosphere at sea level and justifies studying the water molecule to explore the possibility of a three-level gain measurement in H_2O with higher gain.

For a possible three-level gain measurement in H_2O, two coupled transitions have been identified. These are the $4_{32} \leftrightarrow 4_{31}$ transition on the 001 ↔ 000 band, and the $6_{33} \leftrightarrow 5_{50}$ transition on the 001 ↔ 020 band. The HF laser line 1 → 0, P(5), is in near resonance with the $4_{32} \leftrightarrow 4_{31}$ transition of the 001 ↔ 000 band in H_2O. The gain may be measured on the $6_{33} \leftrightarrow 5_{50}$ transition on the 001 ↔ 020 band either with a CW diode laser or with a CW H_2O laser. The salient features of this scheme are presented in Fig. 6. Here several points should be noted. First, the calculated gain at 28 μm turns out to be slightly larger than the 4.3 μm gain measurement in CO_2 (Fig. 3). However, this gain is only for tropical atmospheres at sea level. As one moves to other model atmospheres, the gain decreases. Furthermore, at higher altitudes, the concentration of H_2O in air decreases and so does the gain. For instance, as shown in Fig. 7, at an altitude of 6 Km, we can only obtain a gain of 0.001 cm^{-1} for tropical atmospheres. Thus, this scheme becomes increasingly unattractive as the altitude increases.

The other drawbacks of this scheme are: (i) the gain is measured at longer wavelengths (28 μm) where detector sensitivity is lower yet; and

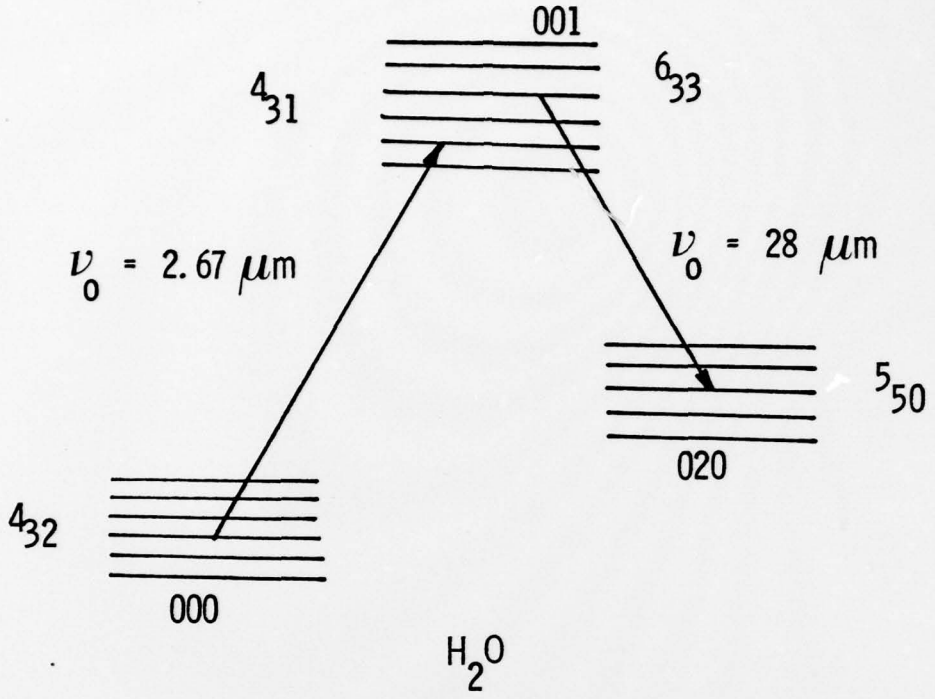

	Pump Laser Characteristics	Probe Laser Characteristics
Type	HF Pulsed Laser	CW H_2O Laser or CW Diode Laser
Laser frequency	2.67 μm (1 → 0 P(5))	28 μm
Absorption/Gain line	H_2O, 000 ↔ 001, $4_{32} \rightarrow 4_{31}$	H_2O, 001 ↔ 020, $6_{33} \rightarrow 5_{50}$
Saturation intensity	> 616 MW/cm^2	---
Pulse duration	≤ 33 nsec	CW
Atmospheric absorption coefficient	0.012 cm^{-1}	≈ 0
Gain at 28 μm	---	0.02 cm^{-1}

Fig. 6 Salient features of 28 μm gain measurement in H_2O.

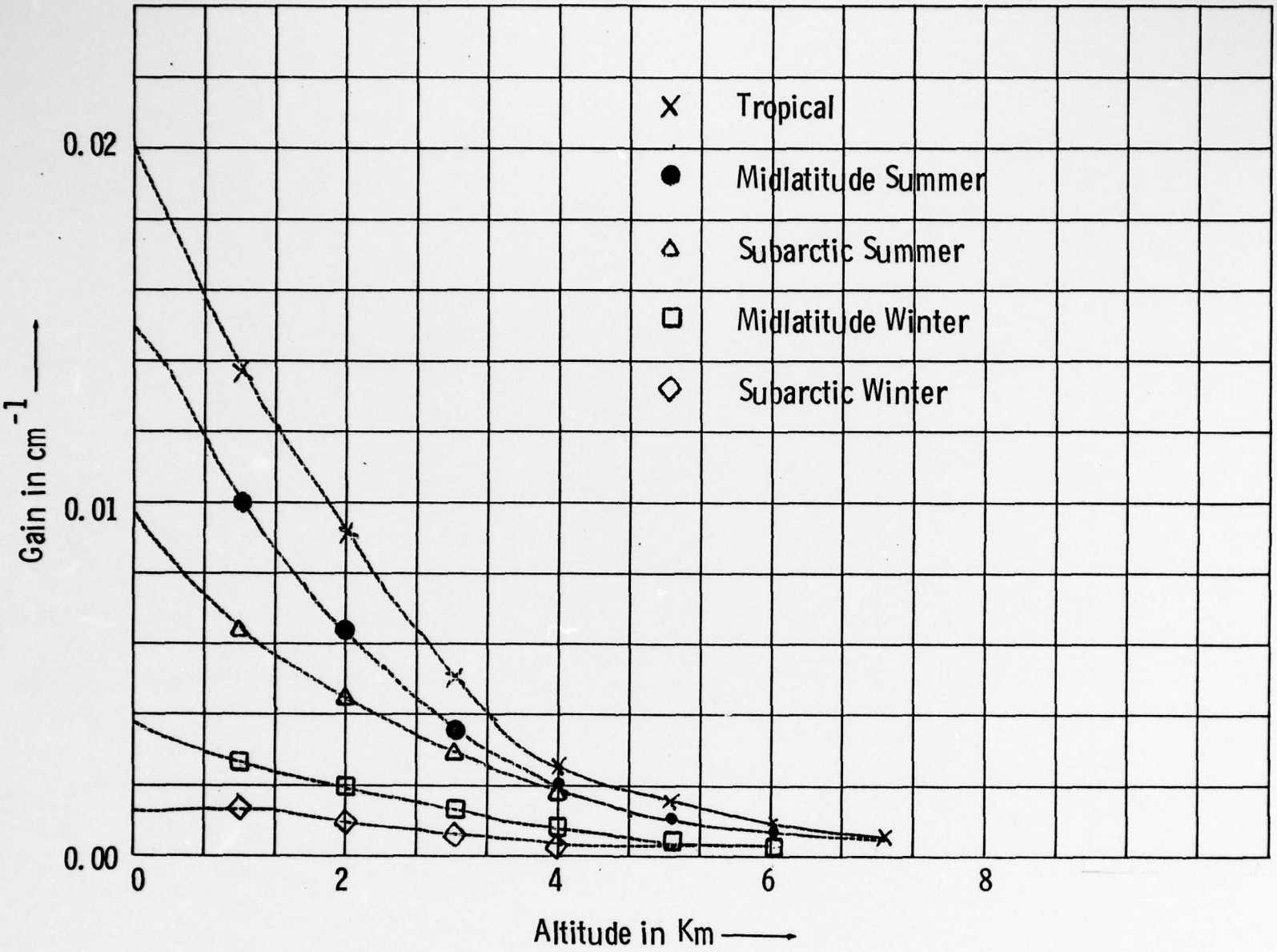

Fig. 7 A plot of three level gain in water vapor vs altitude for five different model atmospheres.

(ii) the laser intensity required to saturate the $4_{32} \leftrightarrow 4_{31}$ transition in the 001 $\leftrightarrow$ 000 band is rather large and this intensity may cause breakdown in the air.

A summary of results for the three-level gain measurement schemes are presented in Table 2 for comparison. It is clear from this table that the most promising of all the three-level schemes is the one which involves pumping the R(12) line of the 021 $\leftrightarrow$ 000 band in CO_2 with an HF laser and the gain measurement on the P(16) line of the 021 $\leftrightarrow$ 020 band with a CW diode laser. In the next section, we will discuss those schemes which monitor parameters other than gain to yield information about turbulent density fluctuations.

TABLE 2

A summary of results on three level gain measurement schemes

PUMP LASER CHARACTERISTICS						PROBE LASER CHARACTERISTICS			
Molecule	Pump Laser	Absorption Line	Laser Pulse Time	Laser Intensity (Saturation)	Absorption Coefficient	Gain Line	Probe Laser	Absorption Coefficient	Gain cm^{-1}
CO_2	HB_r $2 \rightarrow 1$ P(6) 2364.346	CO_2 $001 \rightarrow 000$ R(20) 2364.108	≤ 0.6 μsec	>0.11 MW/cm^2	$0.03\ cm^{-1}$	CO_2 $001 \rightarrow 100$ P(16) 10.6 μm	CW CO_2 Laser	≈ 0	2×10^{-4}
H_2O	HF $1 \rightarrow 0$ P(5) 3741.675	H_2O $001 \rightarrow 000$ $4_{32} \rightarrow 4_{31}$ 3741.306	$\leq$ 33 nsec	>616 MW/cm^2	* $0.012\ cm^{-1}$	H_2O $001 \rightarrow 020$ $6_{33} \rightarrow 5_{50}$ 27.97 μm	(i) CW Diode Laser (ii) CW H_2O Laser	≈ 0	* $0.02\ cm^{-1}$
CO_2	HB_r $2 \rightarrow 1$ P(5) 2382.370	CO_2 $001 \rightarrow 000$ R(54) 2382.507	≤ 0.6 μsec	>1.87 MW/cm^2	1.9×10^{-3}	CO_2 $001 \rightarrow 000$ P(24) 4.294 μm	CW Diode Laser	$0.46\ cm^{-1}$	7.67×10^{-3}
CO_2	HF $2 \rightarrow 1$ P(4) 3622.663	CO_2 $02^01 \rightarrow 00^00$ R(12) 3622.492	≤ 0.6 μsec	>10 MW/cm^2	1.71×10^{-4}	CO_2 $02^01 \rightarrow 02^00$ P(6) 4.32 μm	CW Diode Laser	7.5×10^{-4}	$0.0174\ cm^{-1}$

*For Tropical Atmosphere at Sea Level

3. OTHER DENSITY FLUCTUATION DIAGNOSTIC TECHNIQUES

In this section, we consider those techniques which monitor parameters other than small signal gain to obtain information about the density fluctuations in a turbulent boundary layer. In this category, two schemes have been examined. The first is the use of laser induced air breakdown as a diagnostic tool and the second is the ultra violet-visible fluorescence probes to monitor turbulent density fluctuations. Both these schemes are discussed below.

3.1 The Use of Laser Induced Air Breakdown as a Diagnostic Tool

The breakdown of a gas from the radiation of a focused TEA laser is now a common laboratory phenomenon, occurring at a range of different laser wavelengths, pressures, intensities and gases.[15,16] Many of the studies of this breakdown have been concerned with the complex mechanisms that initiate the breakdown by supplying the initial electrons that are accelerated by the field in the cascade process. This breakdown of the gas may be broken up into several temporal regimes. The initiation of the breakdown is dependent upon the presence of at least one electron within the focal volume. The multiphoton processes responsible for the creation of this 'lucky electron" are still a subject of both theoretical and experimental investigation, and the differences between breakdown in "clean" and "dirty," or laboratory air are, in large part, explained by the presence of impurities capable of easily donating electrons to start the cascade process. Once present, an electron will be accelerated by the intense field in the focal volume of the laser to gain sufficient energy to ionize a neutral particle. This results in the production of two low energy electrons that are again subsequently accelerated in the field. This process repeats itself leading to a high degree of ionization in an extremely short time. In the analysis that follows, we shall be concerned only with the cascade process rather than multiphoton processes that may be of importance during the early stages of ionization.

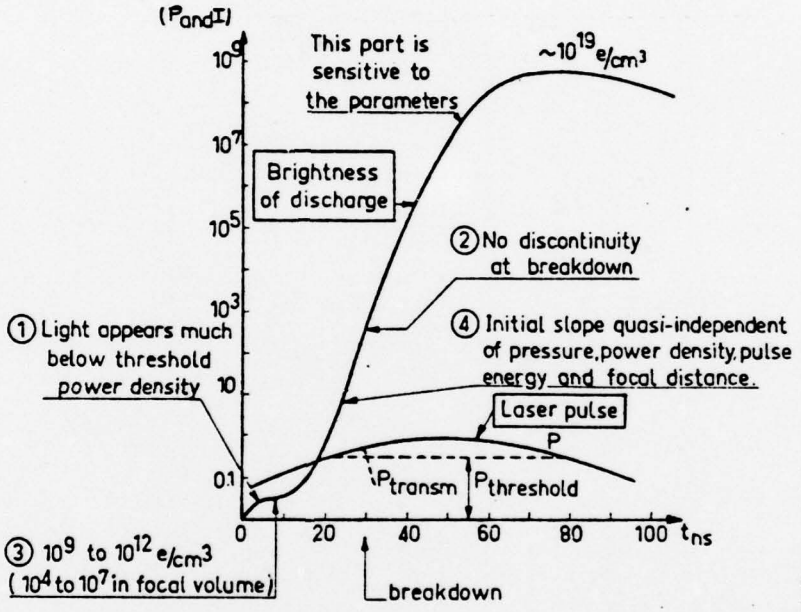

Fig. 8 Summary of observations for a pressure of order 1 atm. Vertical scale for I and P is arbitrary. This figure has been taken from Ref. 17.

In Fig. 8 we see the qualitative behavior of air breakdown at a pressure of nearly one atmosphere.[17,18] For higher laser fluxes, an order of magnitude or more above threshold, and for clean N_2,[19] the breakdown is one to two orders of magnitude more rapid. The purpose of the following investigation will be to examine the dependence of electron density upon neutral density, time, and laser flux during the initial stages of breakdown.

In Fig. 9 we see a possible arrangement by which plasma breakdown and a measurement of the time to opacity or complete ionization can give information on the spectral density and frequency of density fluctuations. At this point we will merely note the well known correlation between spatial measurements of a fluctuating quantity at a single instant of time and the temporal fluctuation (the actual quantity desired) at one point in space.[19] In our proposed experimental configuration, we attempt to remove the one disadvantage associated with using laser breakdown to obtain quantitative information on local properties, and that is the shot to shot variation of the TEA laser itself.

In the configuration indicated, the pulse from the TEA laser passes through a 50% beamsplitter. At each focal point, a breakdown will occur, and the degree of ionization will be such as to severely attenuate the CW CO_2 probe laser passing through these focal points. It is the "time to opacity" measured at detectors 1 and 2 that will provide information on the local state of the gas in the breakdown volume. The measurements must be made as we shall see below, in the order of tens of nanoseconds, which will still ensure that we are concerned with small, i.e., "point" volumes of gas. With additional great attention placed upon obtaining high beam quality, this will minimize the differences in intensity between focal points 1 and 2. Thus, any shot to shot variation in the pulse will manifest itself in the same manner at each breakdown region. A stable CW probe laser, also CO_2, passes through the other side of the beamsplitter as shown. This will cause the probe laser to pass through each focal region. If the second mirror and lens, as well as the second detector were on an optical rail, then the second focal point could be moved easily to measure the spatial correlations of the breakdown times without a need to realign either laser. Each detector will monitor the

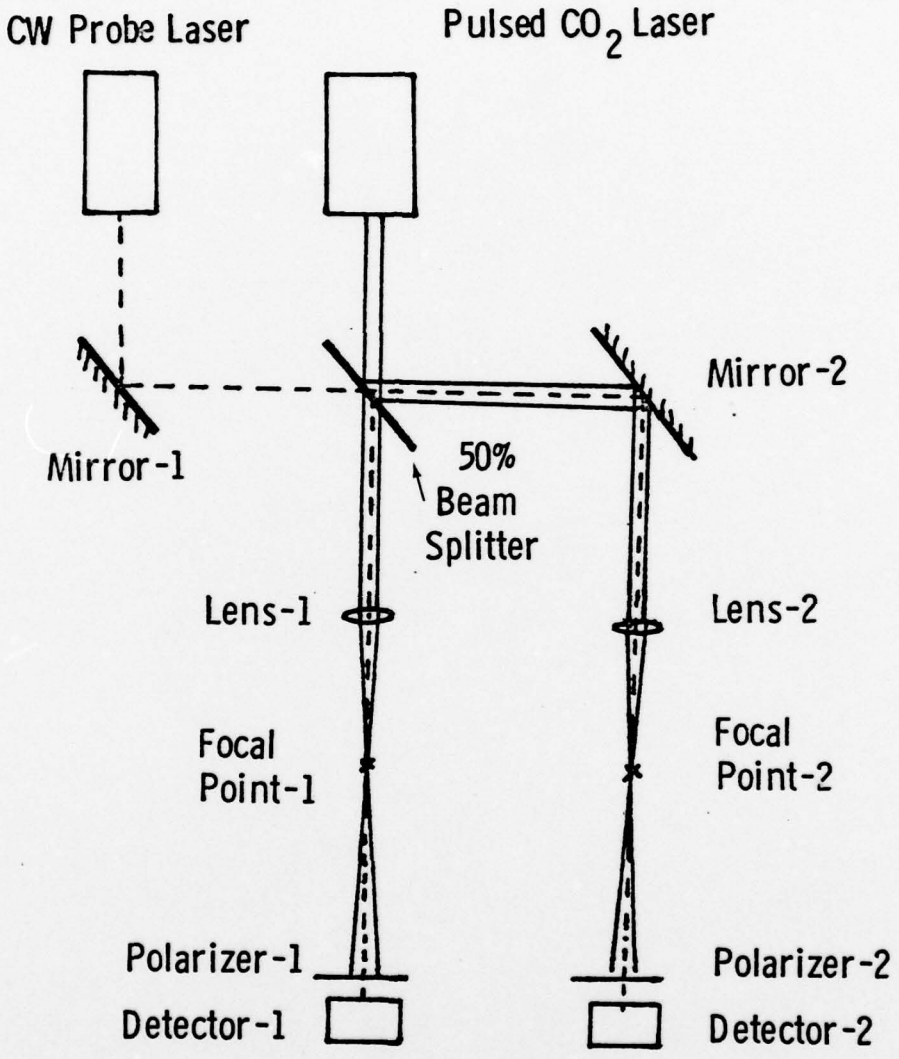

Fig. 9 Experimental configuration for density measurement using gas breakdown.

time required to reach opacity, and it will be shown how the difference in time required to reach full ionization at focal points 1 and 2 will be a sensitive measure of the difference in local neutral particle density. In order to insure that the detectors sample only the CW radiation, we can arrange that the CW laser has polarization different from that of the pulsed laser, and that a suitable polarizer be placed before each detector. The following order of magnitude analysis will provide an estimate of the time required to reach opacity, (i.e., the density associated with the local plasma frequency) and the sensitivity of this rise time to the local particle density.

3.1.1 Order of Magnitude of the Time Required To Reach Opacity

The plasma frequency ω_p depends upon the number of free electrons present that interact with radiation of a given frequency. When the plasma frequency is above or of the order of the laser frequency, significant absorption results. The time to reach this state is what we have called above the "time to opacity." Thus, $\omega_p = 5.64 \times 10^4 (n_e)^{\frac{1}{2}}$, where ω_p is in rad/sec, and n_e in electrons/cm^3. For 10.6 micron radiation, $\omega = 2\pi c/\lambda = 1.77 \times 10^{14}$ rad/sec. For $\omega_p \approx \omega$, $n_e \approx 10^{19}$ electrons/cm^3. Thus, at one atmosphere, complete ionization produces an electron density that corresponds to the plasma frequency. The time to yield this required number of electrons, and the dependence of the electron concentration upon the initial neutral density will be estimated in the following.

We consider first the full energy balance describing the energy increase of the electrons

$$\frac{d}{dt}\left(\frac{3}{2} k T_e\right) = \frac{\left(K_a + K_i\right)_I}{n_e} - \frac{E^*}{n_e} \frac{d n_a^*}{dt} - \left(I_p + \frac{3}{2} k T_e\right) \frac{d n_e}{dt} \qquad (4)$$

$$- \frac{3}{2} k \left(T_e - T_n\right) f \left(\frac{2m}{M}\right)$$

where κ_a is the free-free absorption coefficient for neutral particles, I is the laser flux, and κ_i is the ion absorption coefficient. The electron density is given by n_e; n_a^* is the excited level number density with energy E^*; n_a is the neutral density; I_p is an effective ionization potential; m is the mass of an electron and M is the mass of a neutral. We neglect κ_i compared with κ_a, true certainly until the ionization becomes appreciable. Further,

$$\kappa_a = \frac{e^2 n_e f}{\pi mc\nu^2} \text{ cm}^{-1} \tag{5}$$

where f is the neutral-electron collision frequency. Considering only processes that create electrons in Eq. (4), we may write, as an order of magnitude approximation,

$$\frac{\Delta E}{\Delta t} \sim \frac{e^2 fI}{\pi mc\nu^2} . \tag{6}$$

From this[20] the number of collisions required to raise the energy of an electron by $h\nu$ is approximately

$$\frac{h\nu^3 \pi mc}{e^2 I} . \tag{7}$$

Since we wish the avalanche process to be relatively slow, we choose a threshold laser intensity of $I = 2.8 \times 10^9$ watts/cm^2. For a 10.6 micron photon, $\nu = 2.8 \times 10^{13}$ and for the intensity cited above, we find approximately 2 collisions are needed for an energy increase by $h\nu$. Thus, if we take O_2 as the air constituent with the lowest ionization potential (12.3 ev), and we neglect NO (ionization potential 9.6 ev) the number of collisions

required to raise a neutral particle to the ionization potential is given by Eq. (7), multiplied by 12.3 ev/hν $\simeq$ 100, or 200 collisions necessary to ionize an O_2 molecule. Using data from Phelps and Hake[22] for O_2, we find that $f \approx 8.4 \times 10^{10}$ collisions/sec. at $T_{eo} \approx 300^{o}K$. Thus, 200 (collisions/electron pair)/ 8.4×10^{10} (collisions/sec.) $\approx 2.3 \times 10^{-9}$ sec, the time to create one electron pair. If we consider the avalanche to begin when we have reached $10^9 - 10^{10}$ electrons/cm^3, (see Fig. 8) then we must estimate the time required to increase this original number of electrons to an electron density corresponding to the plasma frequency for 10.6 micron radiation, i.e., 10^{19} electrons/cm^3. If we begin with 10^9 priming electrons/cm^3 then the number of generations of electrons is given as $2^n \approx 10^{19}/10^9$. For this case n = 33 generations of electrons. If we begin with 10^{12} electrons, then the number of generations needed to produce 10^{19} electrons is 23. Thus, between 23 and 33 generations of electrons are needed to reach full ionization with the above intensity and for 10.6 micron radiation. With one generation of electron pairs requiring approximately 2 ns, then we are considering the time to breakdown, again for the conditions specified here, of the order of 45-65 nsec. It should be noted that use of plasma opacity as a fast "shutter" requires an intensity two orders of magnitude larger than specified here, and consequently, the rise time is sub nanosecond.[18] We thus estimate that the experiment proposed will occur on a time sale of the order of several tens of nanoseconds, well within the reach of a modern oscilloscope. A more quantitative estimate of the dependence of this rise time on the neutral density will be conducted in the following subsection.

3.1.2 Dependence of Rise Time on Neutral Density

Variations in the output power of the laser causing the breakdown, as well as variations in the neutral density of the medium in which the breakdown occurs, will cause the time to reach opacity to vary. We will also see that the dependence upon initial electron density (assuming that the threshold condition is satisfied) will be relatively slight. That is, as noted above, a change in the number of priming electrons/cm^3 from 10^{12} to 10^7 only changes the time to reach complete ionization by a factor of two.

We now consider the equation for electron conservation, in standard notation,

$$\frac{dn_e}{dt} = \alpha_I n_a n_e - \beta n_e^2 n_i . \tag{8}$$

Since we are considering processes that will produce the fastest possible rise time, we neglect all loss terms in the energy equation, Eq. (4). We will do the same for the continuity equation, although an iterative procedure on the loss term in the electron continuity equation could easily be employed. With this simplification, the energy equation for electrons becomes

$$\frac{d}{dt}\left(\frac{3}{2} k T_e\right) = \frac{\kappa_a I}{n_e} = \frac{e^2 f I}{\pi m c\nu^2} \tag{9}$$

where f (T_e) is a function of time. In principle, the laser flux, I, may also be a function of time. With the neglect of loss processes to establish a lower bound on the time to opacity, certainly valid until an appreciable fraction of the neutral particles are ionized, we uncouple the electron energy and continuity equations. We assume that the effective collision frequency is proportional to a mean electron velocity[22] and that $f \sim (kT_e)^{\frac{1}{2}}$. For convenience, we will also choose a reference frequency and temperature to enable us to write

$$f = \left(\frac{T_e}{T_{e_R}}\right)^{\frac{1}{2}} f_R . \tag{10}$$

Eq. (7) may now be written as

$$\frac{d}{dt}\left(\frac{3}{2} k T_e\right) = \frac{e^2 f_R}{\pi m c \nu^2}\left(\frac{T_e}{T_{e_R}}\right)^{\frac{1}{2}} I , \tag{11}$$

and may be directly integrated to yield the following:

$$T_e^{\frac{1}{2}} = T_{e_o}^{\frac{1}{2}} + \left(\frac{e^2 f_R}{3\pi m c \nu^2 T_{e_R}^{\frac{1}{2}} k}\right)\int_o^t I(t')\, dt' . \tag{12}$$

This, in principle, allows consideration of pulse shapes upon the increase of the electron temperature. In the following, however, we will restrict the analysis to the case in which the pulse is time independent. Therefore,

$$T_e = \left[T_{e_o}^{\frac{1}{2}} + \frac{e^2 f_R I t}{3\pi k m c \nu^2 T_{e_R}^{\frac{1}{2}}}\right]^2 \tag{13}$$

with $f_R \sim n_a$, we see that as soon as the electron temperature is notably above the initial electron temperature,

$$T_e \sim n_a^2 I^2 t^2 . \tag{14}$$

We now investigate the dependence of the electron density upon electron temperature. Loss terms in the electron density equation are omitted, and we note[20] that

$$\alpha_I = \sigma_e \langle v_c \rangle \left(\frac{I_p}{kT_e} + 2 \right) e^{-I_p/kT_e} \tag{15}$$

with $\sigma_e \sim T_e$ and $\langle v_e \rangle \sim T_e^{\frac{1}{2}}$. Again, choosing a reference temperature, T_{e_R}' (not necessarily the same as previously), we write

$$\frac{\alpha_I}{\alpha_R} = \left(\frac{T_e}{T_{e_R}'} \right)^{\frac{1}{2}} \frac{\exp(-I_p/k\,T_e)}{\exp(-I_p/k\,T_{e_R}')} = \frac{f_I}{f_{I_R}} . \tag{16}$$

The equation for the increase of electron density may now be written as

$$\frac{d\,n_e}{dt} = \left[n_a \alpha_{I_R} \right] \left[\left(\frac{T_e}{T_{e_R}'} \right)^{\frac{1}{2}} \frac{e^{-I_p/kT_e}}{e^{-I_p/kT_{e_R}'}} \right] n_e \tag{17}$$

or

$$\frac{d\,(\ell n\, n_e)}{dt} \sim n_a T_e^{\frac{1}{2}} e^{-I_p/kT_e} .$$

The strong non-linearities of these initial cascade processes are immediately evident. We formally integrate this expression to obtain

$$\ell n\left(\frac{n_e}{n_{e_o}}\right) = \left[\frac{n_a \alpha I_R}{\sqrt{T'_{e_R}}\, e^{-I/kT'_{e_R}}}\right] \int_o^t T_e^{\frac{1}{2}}\, e^{-I_p/kT_e}\, dt' \qquad (18)$$

where, in general, $T_e(t)$ is given by Eq. (13). For the specific case in which we regard I as a constant, a change of variables in Eq. (18) is useful.

$$\int_o^t T_e^{\frac{1}{2}}\, e^{-I_p/kT_e}\, dt' = \int_{T_{e_o}}^{T_e} T_e'^{\frac{1}{2}}\, e^{-I_p/kT'_e}\, \frac{dt'}{dT'_e}\, dT'_e .$$

When dt'/dT'_2 is substituted from Eq. (9), a particularly simple form of the electron density equation becomes

$$\ell n\left(\frac{n_e}{n_{e_o}}\right) = \left[\frac{3\pi k m c \nu^2 f_{I_R}}{2 e^2 f_R I e^{-I_p/kT'_{e_R}}} \left(\frac{T_{e_R}}{T'_{e_R}}\right)\right]^{\frac{1}{2}} \int_{T_{e_o}}^{T_e} e^{-I_p/kT'_e}\, dT'_e . \qquad (19)$$

This integral may be evaluated in terms of elementary functions, and the exponential integral. First, however, we define

$$A \equiv \frac{3\pi k m c \nu^2 f_{I_R}}{2 e^2 I e^{-I_p/kT'_{e_R}} f_R} \left(\frac{T_{e_R}}{T'_{e_R}}\right)^{\frac{1}{2}} \neq f(n_a) \qquad (20)$$

$$X \equiv \frac{I_p}{k T_e} , \quad X_o \equiv \frac{I_p}{k T_{e_o}}$$

with these expressions

$$\ell n \left(\frac{n_e}{n_{e_o}}\right) = A \left\{ \frac{X_o}{X} e^{-X} - e^{-X_o} - X_o \left[E_1(X) - E_1(X_o) \right] \right\} \qquad (21)$$

and

$$X = \frac{1}{\left[X_o^{\frac{1}{2}} + Bt \right]^2} \qquad (22)$$

with

$$B \equiv \frac{e^2 f_R I}{3\pi m c \nu^2 \left(T_{e_R} I_p R \right)^{\frac{1}{2}}} \sim n_a I \quad . \qquad (23)$$

For $I_p >> kT_{e_o}$, we have $1/X_o << 1$. Thus, we may neglect e^{-X_o} and $E_1(X_o)$, and we obtain

$$\ell n \left(\frac{n_e}{n_{e_o}}\right) = X_o A \left[\frac{e^{-X}}{X} - E_1(X) \right] \qquad (24)$$

with A independent of the neutral particle density, n_a, and inversely proportional to the laser flux, I. Thus, for times at which the electron temperature is notably higher than the initial cool gas, i.e.,

$$T_{e_o}^{\frac{1}{2}} << \frac{e^2 f_R I_t}{e \pi m c \nu^2 T_{e_R}^{\frac{1}{2}} k} \qquad (25)$$

we have,

$$\ell n \left(\frac{n_e}{n_{e_o}}\right) \sim \left[t^2 n_a^2 \; I \; e^{-\left(\frac{k}{n_a^2 I^2 t^2}\right)} - \frac{k_1}{I} \; E_1 \left(\frac{k}{n_a^2 I^2 t^2}\right) \right] \qquad (26)$$

For typical values of fluxes and pressures near atmospheric, the first term will dominate, and the exponential term quickly approaches its asymptotic value; thus, our final simple result is characterized by a stronger dependence upon neutral density than upon the laser flux. If we now wish to consider the detector responses of the schematic experiment in Fig. 9, we may make these measurements at two locations simultaneously since the same pulse is causing breakdown at two separate points. The maximum decrease of the signal will be a direct measurement of the integrated electron density through the plasma, and the time at which the two signals decrease relative to one another can be monitored accurately.

$$\frac{\ell n \left(\frac{n_e}{n_{e_o}}\right)_1}{\ell n \left(\frac{n_e}{n_{e_o}}\right)_2} = \frac{\left(n_a\right)_1^2}{\left(n_a\right)_2^2} \qquad (27)$$

where the subscripts 1 and 2 refer to simultaneous measurements of the attenuation of the probe beams passing through the two focal points. Thus, by monitoring the relative intensities just before opacity is reached, it would seem that a sensitive measurement of the densities (neutral) at the two different focal points can be made. The problem

of fluctuation of the shot to shot laser pulse now poses no problem, and the dependence upon the initial electron density (assuming threshold can be reached) is weak. We should also note that a more complete analysis retaining loss terms may give a somewhat weaker density dependence, nevertheless, an exponential dependence is still to be expected.

3.1.3 Conclusions

It is well known that a TEA laser pulse can ionize gas at some distance, and that the rise time of the electron density is a function of several variables, the laser flux, the neutral density, the initial electron density, and the ionization potential being among the most important. One of the drawbacks in attempting to use such a breakdown to obtain quantitative information on the state of the gas, is that fluctuations in the power output of the TEA laser may well be larger than the changes in the state of the gas from point to point in the flow field. With the use of a beam splitter to assure that at each shot, essentially the same shape of the pulse is causing the breakdown, this problem can be avoided. Our calculations indicate that this method may also have a relatively high degree of sensitivity.

3.2 Ultraviolet - Visible Fluorescence Probes to Monitor Density Fluctuations

There are four potential sources of photoexcitation which may yield a fluorescence signal containing information about turbulent density fluctuations. These are: laser-induced fluorescence, laser-induced photodissociative excitation, two-or three-photon photodissociative excitation, and chemiluminescent reaction following photolysis. In the following, we will examine each of these options briefly, after setting initial limits on reasonable signals to guide our choice.

As explained in Section 4 of this report, to achieve 10% precision in the measurement of 1% density fluctuation, 10^6 photons must be detected. If the detector system consists of a collection lens at f/5, an interference filter of 50% transmission and a photomultiplier of 20% quantum efficiency, then 4×10^9 photons must be emitted in the region of interest in order to detect 10^6 photons. If we neglect photon losses resulting from electronic quenching, (an assumption which is valid for all atmospheric quenchers except N_2, O_2 and H_2O even at gas kinetic quenching efficiency), and assume that we are interested in sampling a volume of 2.5×10^{-1} cm^3 (a volume roughly 6.3 mm on a side), then we must have excited-state densities in the viewing region of 1.6×10^{10} particles $cm.^{-3}$ Thus, any species in the atmosphere whose abundance is less than this can immediately be eliminated from consideration.

In order to minimize losses from quenching and convection out of the field of view, candidate fluorescent species should have a radiative lifetime less than 2μs. This requirement essentially restricts the candidate species to atoms, diatomic, and perhaps a few triatomic molecules. In considering species in the normal atmosphere, and possible fragments which could be produced from these species in photolysis, we can find only two possible fluorescense candidates. Molecular oxygen might be observed by laser-induced fluorescence on the Schumann-Runge bands in the ultraviolet. Fluorescence from OH might be observable in two-photon photodissociative excitation of H_2O.

The output of an ArF laser at 193 nm overlaps the P (15, 17, 19) and R (17, 19, 21) lines in the v'=4 to v"=0 transition of the $O_2 B^3\Sigma_u^- - X^3\Sigma_g^-$ band.[23] In the thin-target limit with $\Delta\nu_L >> \Delta\nu_{absorber}$ the fractional absorption of laser light by any of these lines is given by

$$A = \frac{\int k_\nu \ell d\nu}{\Delta\nu_L} \qquad \frac{\pi e^2 N \ell f_o}{m_e c^2 \Delta\nu_L} \tag{28}$$

where k_ν is the frequency-dependent absorption coefficient, N is the number density of the absorbing species, f_o is the oscillator strength of the transition of interest, ℓ is the pathlength of the absorption, $\Delta\nu_L$ is the FWHM of the laser line in cm^{-1} and the other symbols have their usual meanings. For the six lines of interest, we get

$$A = \frac{\pi e^2}{m_e c^2} \qquad \frac{N_{O_2} f_o^{band} \ell}{\Delta\nu_L} \qquad \sum_{6 \text{ lines}} \frac{N_J"}{N_v"} \frac{S_J^{J'}}{2J" + 1}$$

where f_o^{band} is the band oscillator strength (3.04×10^{-7} for the (4, 0) band),[24] N_{O_2} is the number density of oxygen (4.8×10^{18} molecules cm^{-3} at sea level), ℓ is 0.1 cm, $\Delta\nu_L$ is 134 cm^{-1} and the terms in the sum reflect the Boltzmann population distribution, and the rotational line strengths of the lines under consideration. We calculate that $A = 7.2 \times 10^{-5}$. If the ArF laser has an output of 50mJ,[22] then 3.6×10^{12} photons will be absorbed in the viewing region.

Not all of the absorbed photons will fluoresce, however. The Schumann-Runge bands of O_2 predissociate, so that only a fraction of the excited states produced in the absorption of the laser light have the potential to fluoresce. The fluorescence efficiency is given by[24]

$$\eta_{f\ell} = \frac{1}{\frac{\tau_{rad}}{\tau_{diss}}} \tag{29}$$

where τ_{diss} is the predissociative lifetime given by

$$\tau_{diss} = \frac{1}{2\pi c \Delta\nu_{diss}} = 1.27 \times 10^{-12} \text{ sec}$$

and τ_{rad} is the radiative lifetime which is 187 ns for $v' = 4$.[25] Thus, in the absence of quenching, the detected fluorescence signal will be the product of the number of photons absorbed, the fluorescence efficiency against predissociation, and the system detection efficiency. We calculate that the detector signal will be 6×10^5 photons, giving a detection precision of 13% for 1% density fluctuations.

It is to be noted that the quenching of the excited states will be unimportant if the ArF laser is able to saturate the transition.[5] However, the commercially available ArF laser does not produce saturation. Therefore, the detection precision may decrease if the quenching rates for the excited states are of the same order as τ_{rad}. In addition, the detection precision will also decrease by approximately a factor of 2 if the measurement is made at an altitude of 10 Km.

The excited-state number density produced from two-photon dissociative excitation is given by[26]

$$\left[A^*\right] = \frac{\gamma I^2}{h\nu} \left[AB\right] \tau_p \qquad (30)$$

where γ is the two-photon absorption cross-section, typically $\approx 10^{-31}$ $cm^4 W^{-1}$, ν is the laser frequency, I is the laser intensity in W cm^{-2}, τ_p is the laser pulse length, and the other symbols have their usual meanings. For an ArF laser delivering 50mJ in 20 ns to a $1.5mm^2$ target, we calculate that the excited-state number density produced will be 1.5×10^{-4} of the number density of the absorbing species. In order to produce excited-state number densities greater than 10^9 particles cm^{-3}, the parent molecule must have a number density greater than 7×10^{12} molecules cm^{-3}, or a mixing ratio greater than 10^{-6}. From Table 1 we find that this restriction limits the possible parent

molecules to N_2, O_2, H_2O, CO_2 and CH_4. In this list, the only likely candidate for photodissociative excitation would be H_2O which might produce OH fragments emitting around 308 nm.

In general, single photon photodissociative excitation requires more energy than can be met by sources which may be propagated through air. Approximately 4 eV would be required to break a chemical bond, and another 3 eV to provide electronic excitation. This amount of energy, 7 eV, can be delivered only by sources with wavelengths shorter than 175 nm, i.e., beyond the Schumann-Runge cutoff in normal air. There are some exceptions to this, of course, such as the photolysis of O_3 at 250 nm to yield electronically excited O (^1D). We cannot think of any exceptions which give fragments with sufficiently short radiative lifetimes to be useful.

In the past few years, much effort has been expended searching for efficient chemiluminescent reactions which produce visible photons. We are unaware of any successes in these endeavors.

In summary, the only sources of uv-vis photoexcitation which might produce sufficient light intensity to allow measurements in the percent range are laser induced fluorescence of O_2 on the Schumann-Runge bands, and two photon photodissociative excitation of H_2O to produce OH fluorescence. Both of these techniques could be tried in the laboratory with a conventional off-the-shelf ArF laser.[28]

4. TURBULENCE CONSTRAINTS

Making measurement in a turbulent environment requires certain spatial and temporal resolution capability in a diagnostic technique. In general, in a turbulent flow, one is interested in obtaining information about the small scale structure and the energy spectrum. The small scale structure in a turbulent flow has a characteristic dimension given by the Kolmogorov microscale,

$$\eta = \left(\frac{\nu_m^3}{\varepsilon}\right)^{1/4} \tag{31}$$

where η is the small scale characteristic dimension, ν_m is the kinematic viscosity of the medium and ε is the rate of turbulent dissipation of energy. Since η is proportional to the one fourth power of ε, the turbulence microscale for a variety of flows of interest range from 0.5 mm to 1 cm. For our application, the density measurements are pertinent to the turbulent flow around a turret mounted on an airplane. It is specified that the spatial resolution required is approximately 1 cm.

In Section 2, we have seen that the most promising three-level gain measurement technique yields a gain of 0.017 cm^{-1}. Now the gain is directly proportional to the density of the medium. Consequently, to measure 1% density fluctuations we require a gain measurement capability of 1.7×10^{-4} cm^{-1}. In order to see how accurately this measurement can be made, we calculate the signal to noise ratio in the next subsection. We also note that wind tunnel testing with air seeded with CO_2 will significantly increase the sensitivity.

4.1 Signal to Noise Ratio

In Section 2 we have seen that the energy constraint on the pump laser requires that the single pulse experiment be completed in a time less than a microsecond. In such a short time, the noise contribution

due to intrinsic design of the detector is small. The background noise due to 300 K black body radiation does not enter in the calculation of signal to noise ratio because we measure the change in the signal and not its absolute value.

Another source of noise which can significantly reduce the magnitude of the signal is the probe laser absorption in the atmosphere. As was calculated in Section 2, the absorption coefficient at the probe laser frequency is 7.5×10^{-4} cm^{-1}. Since the path length for the probe beam is expected to be approximately 1 meter, the probe laser absorption in the atmosphere will be 7.5×10^{-2}. Even 5% fluctuation in this absorption from shot to shot can conceivably wipe out the gain that we are trying to measure.

This problem of the atmospheric absorption of the probe beam can be resolved if we trigger the scope connected to the detector a few microseconds before we fire the pump laser. This arrangement will establish a reference level and when the pump laser pulse arrives, we can just measure the change from this reference line. Since the single pulse experiment is completed in time less than a microsecond and the characteristic time scale of the turbulence is tens of microseconds, there will be no change in this reference line in a few microseconds. From pulse to pulse, however, this reference line will shift, but we can still measure the gain.

Fluctuations in the detected intensity due to photon statistics is another source of noise. This is the most important noise source which limits the spatial resolution of the density measurement scheme. The CW diode laser to be used to probe the saturated medium delivers 0.5 mW at 4.32μm. In 100 nsecs, which is expected to be the time to complete a single pulse experiment, the laser will deliver 1.1×10^{9} photons to the detector. The statistical fluctuations in detected signal is $(1.1 \times 10^{9})^{\frac{1}{2}}$ and, therefore, the ratio of detected intensity fluctuations to the initial intensity called the noise level, is 3.0×10^{-5}. This calculated noise level depends upon the power of the probe laser, the pulse duration of the pump laser and the effective vibration relaxation rate of the excited level in CO_2.

In Fig. 10, we show the S/N ratio as a function of spatial resolution for 1% density fluctuations. It can be seen that in the spatial range of interest to us, 1 cm, the S/N ratio is fairly reasonable. For instance, for a path length of 1 cm, it is anticipated that we can measure 1% density fluctuations to an accuracy of 16%. It is emphasized here that the S/N ratio as calculated above is only approximate and at sea level. At an altitude of 10 Km, this ratio will drop by a factor of 3. However, if the S/N ratio is not adequate to give a reasonably accurate measurement, we can always use a multipass cell and increase the effective path length for gain. In Fig. 10 therefore, we have also presented the S/N ratio for multiple passes through the same saturated volume. As can be seen, a multipass cell allowing the probe beam to pass several times through the excited volume should be sufficient to provide a reasonably accurate measurement of the density fluctuations.

Now we calculate the temporal resolution required to make measurements in a turbulent environment and see if the three-level scheme under consideration can provide such temporal resolution.

4.2 Temporal Resolution

The highest frequency information which can be obtained from a turbulent flow field is characterized by the time scale of the small scale structure. This time scale is given by the Kolmogorov time, τ_k

$$\tau_k = \left(\frac{\nu_m}{\varepsilon}\right)^{\frac{1}{2}} \tag{32}$$

For our application, the value of the turbulent dissipation rate, ε, is not known, but it is believed that the Kolmogorov time is of the order of tens of microseconds. This time scale is longer than the pulse length of the pump laser, which is approximately six tenths of a microsecond as noted in Section 2. Thus, each sample is taken in a time much shorter than that characterizing the fastest flow motion. This means that a particular sample contains all the information about the fastest flow motion at some instant of time. However, that is not enough, and to obtain frequency spectrum information we need to take samples at the rate of tens of thousand samples per

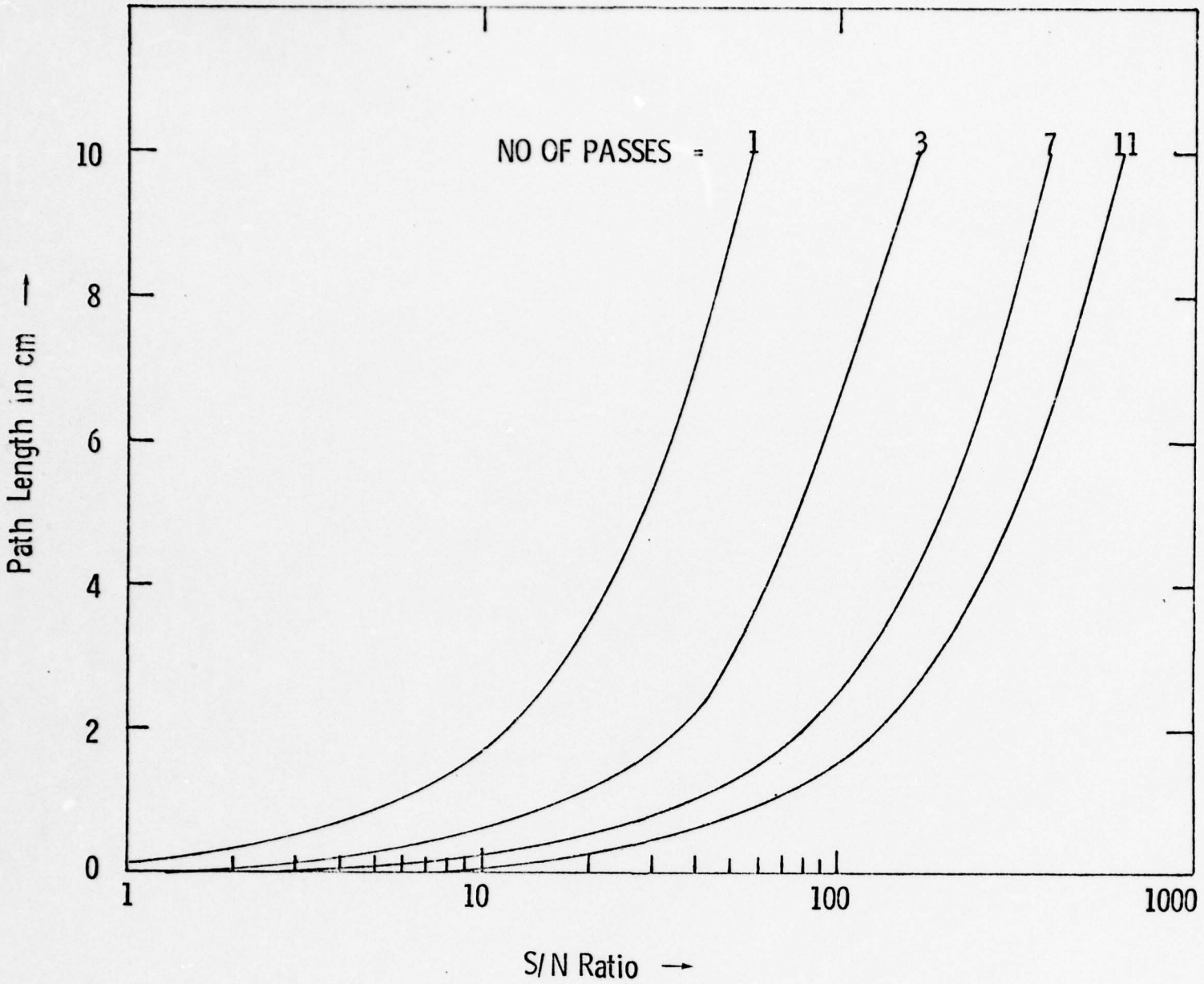

Fig. 10 The S/N ratio for 1% density fluctuations at sea level. At an altitude of 10 Km, this S/N ratio will decrease by a factor of 3.

second. This is because using pulsed devices, we can only recover frequency information up to the Nyquist frequency, which is half the frequency at which the device is pulsed.

The commercially available high power HF lasers delivering power levels of interest to us can provide rep rates of only 1-3 pps. These rep rates are insufficient to provide frequency spectrum information. However, if we assume that the turbulence flow field is random and isotropic, i.e., taking samples at different times is equivalent to taking samples at different points in space, we can obtain information about the fastest flow motion using the commercially available lasers. To see how this is possible, consider Fig. 11. The probe beam is made to pass through a beam splitter which divides the beam into two parts. These parts may not be of equal intensity because we are only interested in the change in intensity. These two parts then serve as two probe beams and sample the saturated gas at two different points in space. By varying the distance between these two beams, we can determine the spatial autocorrelation coefficient, α

$$\alpha \equiv \frac{\overline{\rho(x,t)\ \rho(x+a),\ t}}{\overline{\rho^2}} \tag{33}$$

where a is the distance between the two points where the density measurement is being made at a particular instant of time. If the turbulence is homogeneous, α is only a function of a, i.e. $\alpha = \alpha(a)$. By taking the Fourier transform of $\alpha(a)$, we can obtain the energy spectrum of the fastest flow motion in terms of wave numbers.

From Eq. (33), the power spectrum in terms of frequency can also be obtained if we assume that the turbulence is random. Then the space and time coordinates in Eq. (33) can be interchanged and by taking Fourier transform in frequency space, we can obtain the power spectrum.

If the turbulence in a flow field is not completely random, we may not be able to recover frequency spectrum information but we can always generate probability distribution functions. If N is the total number of

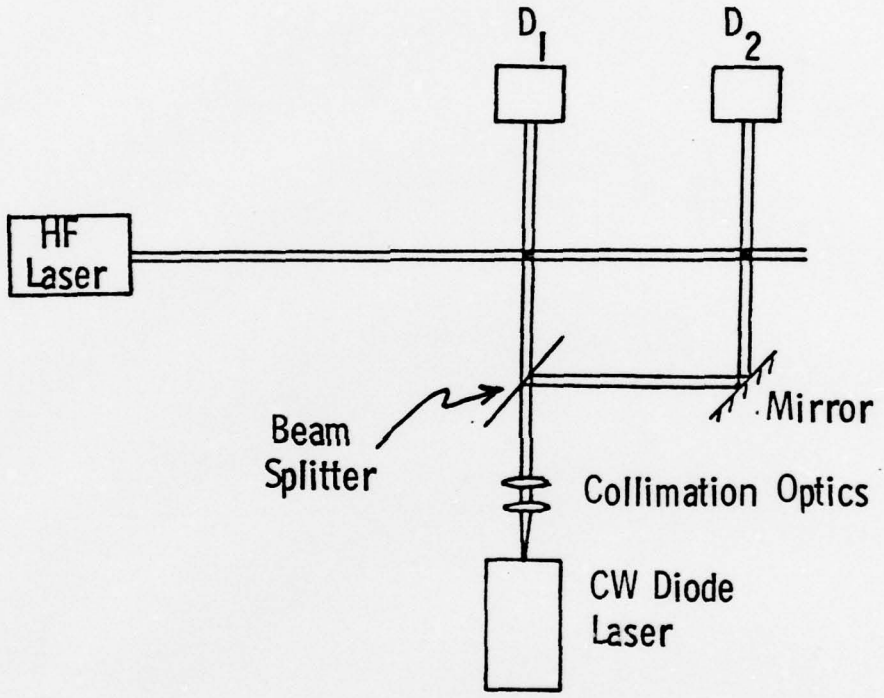

Fig. 11 Experimental configuration which can provide energy spectrum information using low rep rate HF lasers.

density measurements made, and n is the number of measurements that lie between $\rho(t)$ and $\rho(t + \Delta t)$, then the probability density, $B(\rho)$ is defined as

$$B(\rho)\,\Delta\rho \equiv \lim_{N \to \infty} \frac{n}{N}$$

The probability density, $B(\rho)$ satisfies the following normalization condition

$$B(\rho) \geq 0 \,, \quad \int_{-\infty}^{\infty} B(\rho)\, d\rho = 1$$

5. EXPERIMENTAL CONSIDERATIONS

In the first four sections of this report, we have seen that the three-level gain measurement technique which involves using 2.76 μm HF laser for pumping at 4.32 μm can possibly yield useful information about the density fluctuations in a turbulent flow. We have also seen that for 1% density fluctuations, the S/N ratio is such that a reasonably accurate measurement can be made with spatial resolution of 1 cm. In this section, we explore the possibility of performing a simulation experiment in the laboratory.

The HF laser power in $2 \rightarrow 1$ P (4) line needed to saturate $000 \leftrightarrow 021$ band in CO_2 gas must be greater than 10 MW/cm^2, while the pulse length must be less than or equal to six tenths of a microsecond. Two types of high power pulsed HF lasers are available. Both of these models are manufactured by Lumonics Research Limited. One is the Model 210, which can deliver 3.6 MW of total power, and the other is the Model 203, which can deliver 1 MW of total power. The salient features of both of these laser systems are presented in Table 3. The Model 210 has been discontinued by Lumonics Research Limited, but can be obtained custom made at an approximate cost of $40,000. The Model 203 is a modified version of Model 103. At PSI, we have Model 103 and it might be possible to modify this model to obtain 1 MW of power with HF gas.

From Table 3, it can be seen that greater than 6 J/cm^2 fluence for laser line $2 \rightarrow 1$ P (4) can be obtained if the beam is focussed to less than 1.0 mm diameter for Model 210 and 0.5 mm diameter for Model 203. Thus, the available commercial lasers cannot saturate a path greater than 1 mm^2 in cross-section. To obtain a gain length of 1 cm, one may proceed in two ways. First, in the laboratory, the scheme could be tested at a reduced pressure. For CO_2 gas, the collision broadened regime extends down to 10 torr of pressure. In a collision broadened regime, the saturation intensity is directly proportional to the pressure through the vibrational relaxation rate constant. Consequently, by testing the scheme in a wind tunnel at a reduced pressure, say 10 torr (keeping the concentration of CO_2 unchanged), we can relax the

TABLE 3

Relevant Information on Commercially Available High Power HF Lasers

Pump Laser

Type	Lumonics - 210A	Lumonics - 203
Power (multiline)	3.6 MW	1 MW
Power (single line)	0.6 MW	100 KW
Power ($2 \rightarrow 1$ P (4) line)	0.15 MW	25 KW
Beam dia to obtain $6 J/cm^2$	1.0 mm	0.50 mm
Pulse width	0.34 μsec	0.5 μsec
Cost	$ 35 K - 40 K	$ 22 K

requirement on saturation fluence by a factor of 76. This arrangement will permit us to obtain a gain length of approximately 8.7 mm with the Model 210 laser.

The second possibility is to use a cylindrical focussing lens which will permit us to obtain rectangular cross-sections in the focal plane. Focussing the beam to 0.1 mm in one dimension, we can obtain a gain length of 1 cm in the other dimension. This seems a more promising method for obtaining saturation and a cm beam width.

The laser to be used to measure gain at 4.32 μm is the CW diode laser manufactured by Laser Analytics Inc. This laser can be fine tuned to provide a laser frequency which is in resonance with the P(16) line of $021 \leftrightarrow 020$ band in CO_2. The laser operates at cryogenic temperatures and requires a lens assembly to collimate the beam. Definite information about the amplitude stability of this laser over a microsecond time scale is not available, but it is believed that the amplitude stability is better than one part in one hundred thousand during the time of the pumping pulse.

If it is necessary to use a multipass cell to increase the effective gain length, this can also be obtained from Laser Analytics Inc. This multipass cell contains two confocal mirrors placed at two ends of a one meter cell. By appropriately varying the focal lengths of the two mirrors, we can adjust the beam cross-section (in the focal plane) anywhere in the range 1 mm^2 to 1 cm^2. Use of a multipass cell requires transfer optics and it is apparent that the cost of testing the technique will increase.

One advantage of making the gain measurement at 4.32 μm is that sensitive detectors are available in this range of the infrared. Indium antimonide detectors can detect 4.32 μm radiation. These detectors have a rise time of 0.2 μsec and a D* of 10^{11} cm $H_z^{\frac{1}{2}}$ $watt^{-1}$. The noise equivalent power is 10^{-9} watts, which is small in comparison to the power of CW diode lasers.

At PSI, the density fluctuation diagnostic can be assembled and experiments can be performed in gas cells at different pressures to establish gain levels, signal to noise ratio, and determine if the pump laser is

saturating the CO_2 gas. Saturation of the gas is insured if the small signal gain is directly proportional to the CO_2 number density. Then low speed turbulent flow experiments (grid turbulence) should be performed. A transonic wind tunnel with a 6" by 6" test section is located in the Division of Engineering at Brown University, and small scale turbulence experiments could be performed using this tunnel. Once these experiments are completed and the features of this measurement technique have been validated, large scale wind tunnel testing should be performed at either NASA or Air Force laboratories.

6. CONCLUSIONS

In this report, several three-level gain measurement schemes have been examined from the point of view of monitoring density fluctuations in a turbulent environment in the atmosphere. Two other techniques, that of monitoring laser induced fluorescence signal and the use of gas breakdown as a diagnostic tool have also been examined. Our analysis shows that out of all the schemes considered in this report, the three-level scheme which involves using a 2.7 μm HF laser to saturate 000 ↔ 021 band in CO_2 and gain measurement at 10.6 μm with a CW diode laser is the most promising scheme. The pump laser fluence required for saturation comes out to be equal to or greater than 6 J/cm^2 which is achievable with commercially available lasers. Quantitative information about the energy spectrum of the density fluctuations can be obtained by making simultaneous measurements at two different points in space. Furthermore, remote and spatially resolved measurements providing information about the fastest flow motion can be made with reasonable degree of accuracy.

Another technique which has shown some promise of being able to measure 1% density fluctuations in a turbulent environment is the monitoring of laser induced fluorescence of O_2 on the Schumann-Runge bands. It is recommended that both the schemes mentioned above should be tried in the laboratory prior to field experiments.

We wish to emphasize that even though the various schemes in this report are considered from the point of view of monitoring atmospheric density fluctuations, the three-level scheme, in principle, can also be used to measure species concentration in a variety of other applications. For instance, there is considerable interest in determining the extent of spatial non-uniformities in gain in high power HF lasers. The extension of the three-level scheme to this application is straightforward. Other applications where the three-level scheme may be of interest include the measurement of species concentration in MHD flow channels and in turbulent combustion flows.

APPENDIX I

CALCULATION OF SATURATION INTENSITY

We define the saturation intensity for a given transition as that intensity which results in zero gain (in the limiting sense only) on that transition. In a two-level vibration - rotation transition, the small signal gain is given by Eq. (3). Zero gain implies that

$$G_{(\nu)} = \kappa \Delta N_J = \kappa \left(n_{2,J} - \frac{g_{2,J}}{g_{1,J+a}} n_{1,J+a} \right) = 0$$

or

$$n_{2,J} = \frac{g_{2,J}}{g_{1,J+a}} n_{1,J+a} \qquad \text{(AI-1)}$$

where a = +1, 0, -1 corresponds to P, Q and R branch transitions.

When Eq. (AI-1) is satisified, absorptions and stimulated emission balance one another and no further excitation results with increased pump intensity. Eq. (AI-1) also implies that if level 1 is the ground vibrational level, the collisional and radiative relaxation of excited level (2,J) other than via stimulated emission is negligible.

Now we derive an expression for the laser intensity required to saturate a given rotation - vibration transition. We consider vibrational levels 1 and 2. Within each vibrational manifold is a large number of rotational levels. The rate equations for levels (2,J) and (1, J + a) may be written as

$$\frac{dn_{2,J}}{dt} = -Kn_{2,J} - R\left(n_{2,J} - n_{1,J+a}\right) + \sigma_r \left[\left(\frac{n_{2,J}}{N_2} \right)_{eq}^{m} N_2 - n_{2,J} \right] \qquad \text{(AI-2)}$$

$$\frac{dn_{1,J+a}}{dt} \left(\frac{n_{1,J+a}}{n_1}\right)_{eq}^{m} \quad N_2 + R\left(n_{2,J} - n_{1,J+a}\right) + \sigma_r \left[\left(\frac{n_{1,J+a}}{N_1}\right)_{eq}^{m} \quad N_1 - n_{1,J+a}\right]$$

(AI-3)

Here K is the effective rate constant for vibrational relaxation of level (2,J) via processes other than stimulated emission, R is the stimulated emission rate constant (and it is assumed that the laser is resonant with only one rotational line), and σ_r is the rotational relaxation rate constant. For simplicity, in Eqs. (AI-2) and (AI-3) we have taken degeneracy ratio equal to 1.

The stimulated emission rate constant, R, is proportional to the Einstein B coefficient:

$$R = B_{1,J+a;2,J} \int\left(\frac{I_\nu}{c}\right) \; g\left(\nu, \nu_o\right) \; d\nu \qquad \text{(AI-4)}$$

where $g(\nu, \nu_o)$ is the line shape function and ν_o is the line center frequency.

Summation of Eqs. (AI-2) and (AI-3) over all rotational states yields the rate equations for vibration level 2 and 1.

$$\frac{dN_2}{dt} = -R\left(N_2 - N_1\right) - K N_2 \qquad \text{(AI-5)}$$

$$\frac{dN_1}{dt} = R\left(N_2 - N_1\right) + K N_2 \qquad \text{(AI-6)}$$

Analytical solutions of Eqs. (AI-2) through (AI-6) for population inversion cannot be obtained. However, if we assume that $R, \sigma_r >> K$, we can solve for $(N_1 - N_2)$.

$$\frac{(N_1 - N_2)}{(N_1 - N_2)_{t=0}} = 1 - \frac{2R}{N_1 - N_2}_{t=0} \left[\frac{A_1}{\alpha_1} \left(1 - e^{-\alpha_1 t}\right) + \frac{B_1}{\alpha_2} \left(1 - e^{-\alpha_2 t}\right) \right] \quad \text{(AI-7)}$$

where A_1, B_1 are constants and α_1, α_2 are the two rates given by

$$\alpha_1, \alpha_2 = \left(R + \frac{\sigma_r}{2}\right) \left[1 \pm \left(1 - \frac{2R\sigma_r B_f}{\left(R + \frac{\sigma_r}{2}\right)} \right)^{1/2} \right] \quad \text{(AI-8)}$$

$$B_f = \text{Boltzmann factor} = \left(\frac{n_{2,J}}{N_2}\right)_{eq}^{m} = \left(\frac{n_{1,J+a}}{N_1}\right)_{eq}^{m}$$

The slowest rate for population build up in vibrational level 2, α_2 can be simplified as follows:

$$\alpha_2 = \left(R + \frac{\sigma_r}{2}\right) \left[1 - \left(1 - \frac{2 B_f R \sigma_r}{\left(R + \frac{\sigma_r}{2}\right)^2} \right)^{1/2} \right]$$

$$\frac{2 B_f R \sigma_r}{2\left(R + \frac{\sigma_r}{2}\right)} \xrightarrow{\sigma_r >> 2R} 2B_f R$$

Thus, in the absence of any vibrational relaxation, the steady state in population will be obtained when $2B_f R \ll \sigma_r$. Hence, the condition of population saturation which yield a zero gain on vibration levels 1 and 2 and on any of the rotational lines associated with these two vibration levels is

$$\sigma_2 \gg 2B_f R \gg K \qquad \text{(AI-9)}$$

Comparing this condition with the saturation condition for a two level atomic system ($2R \gg K$), we note that if the rotational relaxation is allowed to occur during the time when the laser radiation is pumping molecules, the stimulated emission rate must be increased by a Boltzmann factor. Thus the intensity requirement to saturate two vibrational levels when only one rotation line is resonant with the laser radiation is much more stringent.

It is to be noted that when $2 B_f R < K$, one can still obtain a steady state population distribution, but in this case, the gain between levels 2 and 1 will not be zero.

Now we check the possibility of satisfying Eq. (AI-9) for molecules of interest to us. For CO_2 at 1 atmosphere, $K \approx 1.6 \times 10^6$ sec^{-1} while $\sigma_r \simeq 6.6 \times 10^9$ sec^{-1}. Thus K and σ_r differ by three orders of magnitude and one can conveniently choose a suitable value of the laser intensity which will satisfy Eq. (AI-9).

We can calculate the lower bound on the laser intensity needed to saturate a vibration - rotation transition (I_s) from the following equation:

$$2 R B_f = K \ .$$

Making use of Eq. (AI-4) and assuming that the laser radiation is a delta function in frequency, we get

$$2 B_f \ B_{1,J+a;2,J} \left(\frac{I_s}{C}\right) g\left(\nu_2, \nu_o\right) = K \ .$$

For a pressure broadened transition, the line shape function is a Lorentzian. Thus,

$$I_s = \frac{16\pi^2 K h \nu_o^3}{2 B_f c^2 A} \qquad \frac{\left[\left(\nu_2 - \nu_o^2\right) + \left(\frac{\Delta\nu_L}{2}\right)^2\right]}{\Delta\nu_L} \,, \qquad \text{(AI-10)}$$

where A is the Einstein coefficient for spontaneous emission.

APPENDIX II

INCREASED INVERSION EFFICIENCY IN OPTICALLY* PUMPED TWO-LEVEL MOLECULAR SYSTEMS

ABSTRACT

It is shown how, under certain circumstances, optically pumping an R branch transition at high J number in a molecular gas may result in a situation in which over half of the particles are in the excited vibrational manifold. This can lead to increased gain in transitions to intermediate lying states and increased fluorescence signal in laser induced fluorescence experiments. In addition, gain can also be obtained on pumping band in transitions which have frequencies smaller than the pump laser frequency. Such an arrangement can be employed to obtain a wavelength shift.

*To be published in Optics Letters, December 1979.

The purpose of this note is to specify conditions in a molecular gas under which more than half the particles in the ground vibrational state may be optically excited to a higher vibrational manifold. In a variety of applications there is strong interest in maximizing the excited state number density: nonlinear saturation spectroscopy with lasers,[29] generation of laser oscillations on coupled transitions in an optically pumped three-level system,[30-33] and monitoring gas density using laser induced fluorescence in a gas flow.[6] In a two-level atomic system, optical pumping can result in the excitation of at most half the lower energy state particles (assuming that the degeneracy of the two levels coupled to the laser radiation is equal). Once the number of particles in the lower and upper level becomes equal, saturation sets in and no further excitation results from increased pump intensity. In a two-level molecular system, however, as a consequence of competing relaxation processes, it will be shown how more than half of the lower vibrational state particles may be excited to a higher vibrational level.

We consider a two-level molecular system with vibrational levels 1 and 2. Within each vibrational envelope is a large number of rotational levels. We assume, for simplicity, that the pumping laser frequency and line width are such that absorption occurs only on one rotational line. In a molecular system, typically, the rotational relaxation rate is 2 - 3 orders of magnitude larger than V-V or V-T energy transfer rates. Consequently, we can obtain, by a proper choice of laser intensity, a characteristic pumping time (τ_p) which is much larger than τ_R but much less than τ_V, where τ_R, and τ_V, are the characteristic times for rotational and vibrational relaxation, respectively. Under these conditions, if the pumping laser is tuned to one rotational line, and if saturation occurs, the population of these two upper and lower vibrational-rotational levels will be equal. However, this condition does not necessarily imply that only half of the total molecules in both vibrational states can be excited to the higher vibrational state.

We consider the following. Let the upper vibrational-rotational level coupled to the radiation be denoted by (2,J). Then the lower vibration-rotational level is (1,J+a), where a = +1, 0, and -1, respectively, corresponds to a P, Q or R branch transition. In the presence of a strong saturating field, the number of molecules in level (2,J) is given by

$$n_{2,J} = \frac{g_{2,J}}{g_{1,J+a}} \quad n_{1,\,J+a} \tag{AII-1}$$

where $g_{2,J}$ and $g_{1,J+a}$ are the degeneracies of levels (2,J) and (1, J+a) respectively. Since $\tau_R \ll \tau_p$, complete rotational equilibrium exists in the vibrational levels 1 and 2. Consequently, the number of molecules $n_{2,J}$ and $n_{1,J+a}$ are given by the Boltzmann distribution

$$n_{2,J} = N_2 \frac{hcB_2}{kT} \quad (2J + 1) \exp \quad \left[- B_2 hcJ(J + 1)/kT\right] \tag{AII-2}$$

$$n_{1,J+a} = N_1 \frac{hcB_1}{kT} \quad \left[2\ (J+a) + 1\right] \quad \exp\left[- B_1 hc(J+2)\ (J+a+1)/kT\right] \tag{AII-3}$$

where N_1, N_2 are the total number of molecules in the vibrational levels 1 and 2 and B_i is the rotational constant. From Eqs. (AII-1), (AII-2) and (AII-3), the ratio of total population in vibrational manifolds 1 and 2, N_2/N_1 can be determined as follows:

$$\frac{N_2}{N_1} = \frac{\exp\ (-\alpha(J + a))}{\exp\ (-\alpha(J))} \tag{AII-4}$$

where

$$\alpha(J) = \frac{BhcJ\ (J+1)}{kT} \qquad \text{(AII-5)}$$

in Eqs. (AII-4) and (AII-5), for simplicity we have assumed that the rotational constants for levels 1 and 2 are equal, i.e., $B_1 = B_2 = B$.

If the total number of molecules is N_o ($N_o \equiv N_1 + N_2$), we can calculate N_2/N_o from Eq. (AII-4) as

$$\frac{N_2}{N_o} = \frac{\exp\ (-\alpha(J+a)}{\exp\ (-\alpha(J+a)) + \exp\ (-\alpha(J))} \qquad \text{(AII-6)}$$

In Figure 12, the ratio N_2/N_o is plotted as function of the Boltzmann factor, BF ($B_f \equiv N_{2,J}/N_2$) for P, Q and R branch pumping in HF and CO. These are merely representative cases and the conclusions drawn in the following pertains to any optically pumped two-level molecular system. It can be seen that for both HF and CO molecules, more than half the particles can be excited to vibrational level 2 if the pump laser is tuned to a high J rotational line on an R-branch transition. In fact, if we pump far enough in the tail of the rotational distribution on an R-branch transition, we can virtually empty the ground state. The important parameter which determines the extent of excitation to level 2 is the rotational partition function, Q_r ($Q_r \equiv \frac{kT}{hcB}$). If Q_r is small, for the same BF, one can excite more particles to the excited level 2 than when Q_r is large. Since Q_r is directly proportional to the temperature, Fig. 12 also shows that it is advantageous to pump a gas at lower temperature in order to increase the excited state number density.

To consider gain on a transition between level (2,J) and a level intermediate between 1 and 2 (and essentially unpopulated thermally), we need only multiply, Eq. (AII-6) by a Boltzmann distribution. We also examine the possibility of gain between vibrational levels 1 and 2. The population inversion

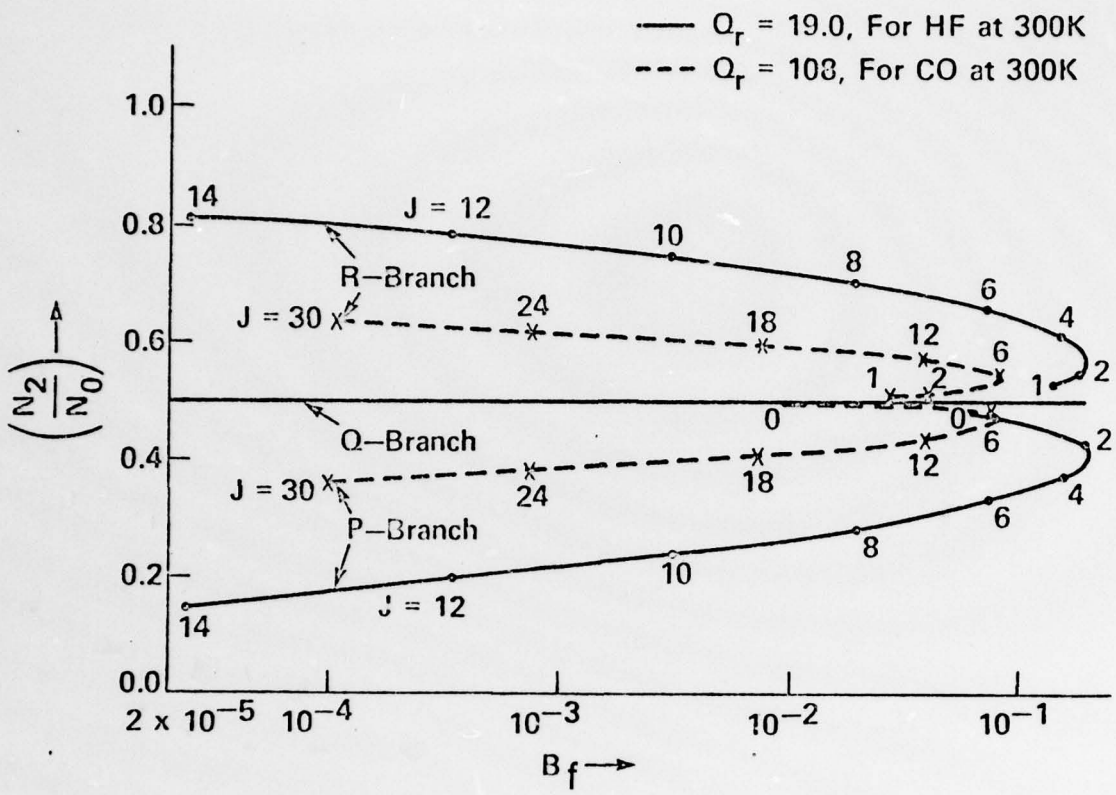

Fig. 12 Normalized excited vibration population as function of the Boltzmann factor, B_f ($B_f = n_2 J/N_2$).

$$\Delta N_{J'} \equiv \left(n_{2,J'} - \frac{g_{2,J'}}{g_{1,J'+a'}} \; n_{1,J'+a'} \right) / N_o$$

where a' = +1, o, -1, for P, Q and R-branch transitions respectively, is given as follows:

$$\frac{\Delta N_{J'}}{N_o} = \left[\frac{(2\,J'+1)\; Bhc \exp(-\alpha(J)) \exp(-\alpha(J'+a'))}{kT \left[\exp(-\alpha(J+a)) + \exp(-\alpha(J))\right]} \right] x$$

$$\left[\exp\left[-\frac{Bhc}{kT} \left[2aJ - 2a'J' + a - a' + a^2 - a'^2 \right] \right] - 1 \right] \qquad \text{(AII-7)}$$

In a thermalized rotational distribution, the population inversion on a P-branch transition is larger than on Q- or R-branch transition. Consequently, for a given rotational partition function, the maximum population inversion is obtained when the rotational level with the most particles in the excited states (J'_{max}) is involved in P-branch transition. In Fig. 13 we show this maximum population inversion normalized by the total number density as function of B_f for P, Q, and R-branch pumping. It can be seen that a very large population inversion is predicted when pumping is done on R-branch transition. One interesting result to be noted from Fig. 13 is that even though P-branch pumping excites less than half the ground state particles to the vibration level 2, one can still obtain population inversions on P-branch transitions having frequency smaller than that of the pump laser. This population inversion, however, is small and is due to the fact that the frequency of P-branch transition decreases as J is increased.

It is to be noted that if the pumping laser is tuned farther and farther away from the maxima of the rotational distribution, the number of particles available in one rotational level keeps on decreasing. Consequently, to

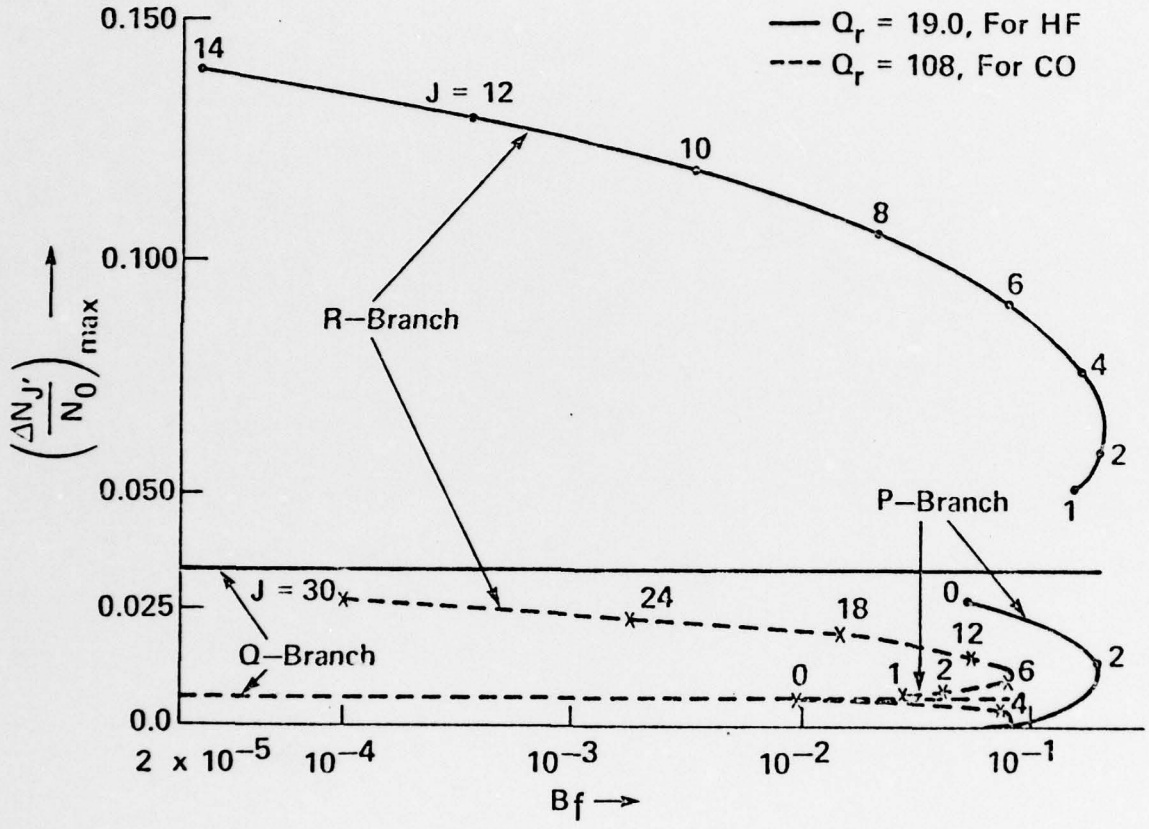

Fig. 13 Normalized maximum population as function of B_f.

cause saturation, the pumping intensity must be increased (Saturation Intensity $\sim$ absorption coefficient $^{-1}$). However, in the collision broadened regime, the saturation intensity is directly proportional to the pressure through the characteristic time for vibrational relaxation. Therefore, in the collision broadened regime, by reducing pressure it is possible to cause saturation at reduced pumping intensity.

The extreme depletion of the ground state as predicted above may be pertinent to studies in the reaction kinetics of excited states. Increased population in the excited state can also lead to an increase in the fluorescence signal in laser induced fluorescence experiments[5] and increased gain in transitions to intermediate lying states. Furthermore, pumping on high J values in R-branch transitions and obtaining lasing on other transitions which have inverted populations can provide us with an efficient method of frequency shifting. This can be applied to the selection of lines that propagate through the atmosphere with less attenuation, and can also be used to shift lines to obtain greater absorption in optical pumping techniques.

REFERENCES

1. S. Lederman, "The Use of Laser Raman Diagnostics in Flow Fields and Combustion," Prog. Energy Combust. Sci. 3, 1-34 (1977).

2. N. A. Chigier, "Instrumentation Techniques for Studying Heterogeneous Combustion," Prog. Energy Combust. Sci. 3, 175-189 (1977).

3. M. Pealot, R. Bailly and J. P. E. Taran, "Real Time Study of Turbulence in Flames by Raman Scattering," Optics Comm. 22, 91-94 (July 1977).

4. S. S. Penner and T. Jerskey, "Use of Lasers for Local Measurement of Velocity Components, Species Densities, and Temperature," Annual Rev. Fluid Mechanics, 5, 9-30 (1973).

5. J. W. Daily, "Laser Induced Fluorescence Applied to Turbulent Reacting Flows." Presented at the Western Section Combustion Institute Meeting, (LaJolla, California, Fall 1976), paper 76-24.

6. A. C. Eckbreth, P. A. Bonczyk and J. F. Verdieck, "Review of Laser Raman and Fluorescence Techniques for Practical Combustion Diagnostics" *United Technology Research Center Report No. EPA-600/7-77-066* (June 1977).

7. M. Lapp, C. M. Penny and J. A. Asher, "Application of Light-Scattering Techniques for Measurements of Density, Temperature, and Velocity in Gas Dynamics," Aerospace Research Laboratories Report No: ARL 73-0045 (April 1973).

8. P. C. Black and R. K. Chang, "Laser-Raman Optical Multichannel Analyzer for Transient Gas Concentration Profile and Temperature Determination," AIAA J, 16, 295-296 (April 1978).

9. R. Goulard, "Laser Raman Scattering Applications," J. Quant, Spectrosc. Radiat. Transfer, 14, 969-974 (1974).

10. S. Lederman, "Some Applications of Laser Diagnostics to Fluid Dynamics," AIAA paper No. 76-21 (Jan. 1976).

11. F. Robben, "Comparison of Density and Temperature Measurement Using Raman Scattering and Rayleigh Scattering," Proceedings of Project Squid Workshop held at Purdue University (December 1975), pp 179-195.

12. R. Beck, W. Englisch and K. Gürs, Table of Laser Lines in Gases and Vapors, Springer Series in Optical Sciences, Vol. 2, pp. 46 (1976).

13. R. A. McClatchey etc., "AFCRL Atmospheric Absorption Line Parameters Compilation," AFCRL - TR - 73 - 0096 (Jan. 1973).

14. R. L. Taylor and S. Bitterman, "Survey of Vibrational Relaxation Data for Processes Important in the CO_2-N_2 Laser System," Rev. Mod. Phys. 41, 26-47 (Jan. 1969).

15. Claudis de Mickelis, "Laser Induced Gas Breakdown: a Bibliographical Review," IEEE J. Quant. Electr., QE-5, p. 188 (April 1969).

16. C. Grey Morgan, "Laser Induced Breakdown of Gases," Rep. Prog. Phys., 38, pp. 621-665, (1975).

17. Renaud Papoular, "The Initial Stages of Laser Induced Gas Breakdown," Laser Interaction and Related Plasma Phenomena edited by H. Hara and H. Schwartz, p. 79, (1971).

18. H. S. Kwok and Eli Vablanovich, "Electrical Triggering of an Optical Breakdown Plasma with Subnanosecond Jitter," Appl. Phys. Lett. 27, pp. 583, (Dec. 1975).

19. J. O. Hinze, Turbulence, second edition, McGraw Hill, pp. 61 (1975).

20. Y. B. Zeldovich and Yu. P. Raizer, Physics of Shock Waves and High Temperature Hydrodynamic Phenomena, Academic Press (1966).

21. R. D. Hake and A. P. Phelps, "Momentum Transfer and Inelastic Collision Cross-Sections for Electrons in O_2, CO and CO_2," Phys. Rev. 158, pp. 70 (June 1968).

22. P. D. Thomas and H. M. Musal, "A Theoretical Study of Laser Target Interaction," Lockheed Report LMSC D 313 142, (Dec. 1972).

23. R. Burnham and N. Djeu, "Ultraviolet-Preionized Discharged-Pumped Lasers in XeF, KrF, and ArF," Appl. Phys. Lett. 29, 707 (1976).

24. J. E. Frederick and R. D. Hudson, "Predissociation Linewidths and Oscillator Strengths for the (2-0) to (13-0) Schumann-Runge Bands of O_2," J. Mol. Spectrosc., 74, 247 (1979).

25. G. Herzberg, Molecular Spectra and Molecular Structure I. Spectra of Diatomic Molecules, 2nd ed., New York: Van Nostrand Reinhold Co., 1950, pp. 405f.f.

26. Calculated from f_{4-0} from Ref. 3 and the v'=4, v". Franck-Condon factors in P.H. Krupenie, "The Spectrum of Molecular Oxygen," J. Phys. Chem. Ref. Data. 1, 423 (1972) p. 490.

27. D. J. Kligler, H_1 Plummer, W. K. Bischel and C. K. Rhodes, "Photolytic Production of $S(^1S)$ from OCS by Two-Quantum and Vibrationally Dependent Mechanisms," J. Chem. Phys. 69, 4652 (1978).

28. Tachisto Inc., Needham, MA.

29. N. Skribanowitz, M. J. Kelly and M. S. Feld, "New Laser Technique for the Identification of Molecular Transitions," Phys. Rev. A6, 2302-2311 (Dec. 1972).

30. T. Y. Chang and O. R. Wood II, "Optically Pumped Atmospheric-Pressure CO_2 Laser," Appl. Phys. Lett. 21, 29-21 (1972).

31. T. Y. Chang and O. R. Wood II, "Optically Pumped N_2O Laser," Appl. Phys. Lett., 22, 93-94 (Feb. 1973).

32. M. I. Buchwald, C. R. Jones, M. R. Fetterman and M. R. Schlossberg, "Direct Optically Pumped Multiwavelength CO_2 Laser," Appl. Phys. Lett., 29, 300-302 (Sept. 1973).

33. J. M. Telle, R. C. Eckhardt and M. S. Sorem, "Efficient, Optically Pumped CF Laser System," 1979 IEEE/OSA Conference on Laser Engineering and Applications, Washington, D. C., (May 1979).